

NATIONAL INSTITUTE FOR FUSION SCIENCE

Statistical Theory and Transition in Multiple-scale-lengths Turbulence in Plasmas

S.-I. Itoh and K. Itoh

(Received - May 15, 2001)

NIFS-703

June 2001

This report was prepared as a preprint of work performed as a collaboration research of the National Institute for Fusion Science (NIFS) of Japan. This document is intended for information only and for future publication in a journal after some rearrangements of its contents.

Inquiries about copyright and reproduction should be addressed to the Research Information Center, National Institute for Fusion Science, Oroshi-cho, Toki-shi, Gifu-ken 509-02 Japan.

RESEARCH REPORT
NIFS Series

Statistical Theory and Transition in Multiple-scale-lengths Turbulence in Plasmas

Sanae-I. Itoh^a and Kimitaka Itoh^b

^aResearch Institute for Applied Mechanics, Kyushu University, Kasuga 816-8580, Japan

^bNational Institute for Fusion Science, Toki, 509-5292, Japan

Abstract

The statistical theory of strong turbulence in inhomogeneous plasmas is developed for the cases where fluctuations with different scale-lengths coexist. Nonlinear interactions in the same kind of fluctuations as well as nonlinear interplay between different classes of fluctuations are kept in the analysis. Nonlinear interactions are modelled as turbulent drag, nonlinear noise and nonlinear drive, and a set of Langevin equations is formulated. With the help of an Ansatz of a large number of degrees of freedom with positive Lyapunov number, Langevin equations are solved and the fluctuation dissipation theorem in the presence of strong plasma turbulence has been derived. A case where two driving mechanisms (one for micro mode and the other for semi-micro mode) coexist is investigated. It is found that there are several states of fluctuations: in one state, the micro mode is excited and the semi-micro mode is quenched; in the other state, the semi-micro mode is excited, and the micro mode remains at finite but suppressed level. New type of turbulence transition is obtained, and a cusp type catastrophe is revealed. A phase diagram is drawn for turbulence which is composed of multiple classes of fluctuations. Influence of the inhomogeneous global radial electric field is discussed. A new insight is given for the physics of internal transport barrier. Finally, the nonlocal heat transport due to the long-wave-length fluctuations, which are noise-pumped by shorter-wave-length ones, is analyzed and the impact on transient transport problems is discussed.

keywords: strong plasma turbulence, Langevin equation, extended fluctuation-dissipation theorem, turbulence transition, cusp type catastrophe, phase diagram, radial electric field, transient transport response

1. Introduction

High temperature plasmas are often in the state far from the thermal equilibrium, and the development of statistical theory for the strongly turbulent plasma has been one of the main subject of plasma physics theory.

One of the characteristic features of strong plasma turbulence is that it is driven by spatial inhomogeneities of plasma parameters and those of fields (*e.g.*, magnetic field and radial electric field) and that it is composed of varieties of modes with different scale lengths. Theories have been developed by use of various methods, *e.g.*, introduction of plasma dielectric in collision integral, renormalized propagator and clump algorithm, scale-invariance method, two-point DIA and $K - \epsilon$ model, shell model, Langevin equation formulation, and others. (See, *e.g.*, reviews in [1-6].) These methods have been successfully used in explaining some aspects of strong plasma turbulence.

In the previous articles [7-12], the statistical theory of subcritically-excited strong turbulence in inhomogeneous plasmas has been developed, based upon the formulation of Langevin equation [13-15]. (Hereafter in this article, references 8-12 are abbreviated as I, II, III, IV and V, respectively.) With the help of an Ansatz of the large degree of freedoms with positive Lyapunov number, the Langevin equation is solved and the fluctuation dissipation theorem in the presence of strong plasma turbulence has been derived. The spectral decomposition is introduced and the Fokker-Planck equation is formulated for fluctuation components. This allows us to calculate the probability density flux, and the transition probability between turbulent states has been obtained. The relation with the thermodynamical limit has been clarified. Obtained formulae are extensions of the Fluctuation Dissipation Theorem (FDT) [16], Prigogine's principle of minimum entropy production rate [17] and the Arrhenius law [18] for the transition probability, which have been employed in the vicinity of the thermodynamical equilibrium.

Analyses in I-V have been applied to a limited case where the turbulence is characterized by one micro scale length (say, the collisionless skin depth $\delta = c/\omega_p$). It is well known that there are many kinds of turbulent fluctuations in high temperature plasmas and that they are characterized by different scale lengths. In particular, the drift wave fluctuations (including ion-temperature gradient mode) whose wave length is of the order of ion gyroradius, ρ_i , are considered to dictate a considerable part of turbulent transport (in particular, for ion energy transport). In general, fluctuations with different scale lengths coexist in plasmas. In order to treat this kind of system, the scale separation is used in the conventional approaches. In addition, in analyzing one class of mode, fluctuations of other scale lengths are often neglected: This simplification is not always relevant, because nonlinear interactions between different-scale-length fluctuations could be important.

Importance of interactions between the modes with different scale lengths has been recognized recently. For instance, the dynamics of meso-scale structure of radial electric field [19] is known to cause varieties in the dynamics of microscopic fluctuations; Examples include the electric field domain interface [19, 20], zonal flow [21] and streamer [22], and an effort to develop a statistical theory for zonal flow is reported [23]. (See [1-3] for recent investigations.) It is necessary to generalize the formalism of statistical theory of turbulence which is developed in I-V in order to analyze this case.

Drift wave fluctuation is usually called as the micro mode (micro-turbulence). Hereafter we call the drift type collective fluctuations as "semi-micro mode" and distinguish it from the "micro mode" of the scale of skin depth. Namely, $\rho_i > \delta$ holds in the system of our concern. The micro-turbulence ($\sim \delta$) is considered to cause the electron anomalous transport as well. In order to consider the anomalous transport, the coexistence of "micro" and "semi-micro" fluctuations and their interplay should be taken into account.

In this article, we extend our framework of statistical theory to include two different collective modes with different scale lengths. Namely, the nonlinear interactions between micro-mode ($\sim \delta$) and semi-micro mode ($\sim \rho_i$) are taken into account. Their interplay (nonlinear dynamics) determines both the fluctuation levels and the cross field turbulent transport. The model and formulations are presented. (Related discussion of the global mode by use of direct numerical simulation is given in [24].) The term "global" is used for the gradient scale lengths of the order of a , and the global parameters (averaged on magnetic surfaces) are given and fixed here. Thermal fluctuation of the order of Debye length, λ_D , is considered as a thermal fluctuation, and is assumed to be statistically independent of the modes of our concern. The effect of thermal fluctuations is included as the collisional drags and the thermal noise of temperature T .

The nonlinear interactions of two collective modes of fluctuations are treated as follows. Nonlinear self-interactions in one class of fluctuation are divided into the coherent drag and the self-noise as has been done in I-V. The micro turbulence of smaller size affects the semi-micro one through the renormalized drag and the "micro" noise. The treatment is analogous to the case of micro turbulence which is affected by the thermal fluctuations of smaller size. On the other hand, the effect of semi-micro turbulence is included in the dynamical equation of the micro-mode as a kind of a driving force or damping force. This is because the spatial structure of semi-micro mode can be large-scale inhomogeneity for the micro-turbulence to be driven or damped. The hierarchical structure is adopted. The combined Langevin equations are to be formulated. A set of equations of the fluctuation level and decorrelation rate for the micro and semi-micro fluctuations is obtained. A case where two driving mechanisms exist (one for micro mode and the other for semi-micro mode) is investigated. It is found that there are several states of fluctuations: in one state, the micro mode is excited and the semi-micro mode is

quenched (although both of them are subject to the drives by global inhomogeneities); in the other state, the semi-micro mode is excited, and the micro mode remains at finite but suppressed level. New type of turbulence transition is obtained, namely, a hard bifurcation can take place between these two states. A phase diagram is drawn, and a cusp type catastrophe is revealed. Turbulence transition which is induced by the shear of global radial electric field is analyzed. A new insight is given for the physics of internal transport barrier.

In some circumstances, the much longer-wave-length components are stable but can be excited by the nonlinear noise of micro mode (and/or semi-micro mode) fluctuations. In this case, the longer-wave-length components induce the heat flux which is not expressed in terms of the local gradient parameters. This kind of heat flux is estimated, and its impact on the transient transport problems [25] is discussed.

The constitution of this paper is the following. In §2, model and basic equations are given. Starting from one model equation of five fluctuating-fields, the nonlinear interactions are formally divided into drags, drives and noises. Then the Langevin equations are reformulated for each collective mode by introducing the scale separation. In the equation, nonlinear interaction terms are modelled as the function of another collective mode. Solving two Langevin equations with some constraints, the correlation functions (fluctuation level, transport quantities) are obtained. The explicit formulae are given for the interplay between the current-diffusive interchange mode (CDIM) [1] of micro-turbulence and the ion temperature gradient (ITG) mode [2] of drift wave type semi-micro turbulence in §3. Possible nonlinear interaction effects are discussed. In §4, the excitation of stable longer-wave-length modes by nonlinear noise of micro (semi-micro as well) mode turbulence is analyzed. The nonlocal heat flux and transient transport are discussed. Summary and discussion are given in §5. Some implication for the change of turbulent transport in internal transport barrier [26] formation is discussed.

2. Basic Equations

2.1 Model

We study a slab plasma, the pressure of which is inhomogeneous in the x - direction, in a sheared magnetic field $\mathbf{B} = (0, sx, 1)\bar{B}_0$. Magnitude of the magnetic field is also inhomogeneous in the x -direction $\bar{B}_0 = (1 + \Omega'x + \dots)B_0$.

A reduced set of equations for the variables $\{\phi, A_{\parallel}, V_{\parallel}, p_e, p_i\}$ is employed for the study of instabilities with multiple scale lengths. ($\phi, A_{\parallel}, V_{\parallel}, p_e$ and p_i are the perturbations of electrostatic potential, vector potential in the direction of main magnetic field, ion velocity in the direction of main magnetic field, electron pressure and ion pressure, respectively.) In this article, we investigate the interplay between the turbulence

in the range of ion gyroradius (say, ion-temperature-gradient (ITG) mode) and those in the range of collisionless skin depth (like current-diffusive interchange mode (CDIM)). The system of fluctuating field variables $\{\phi, A_{\parallel}, V_{\parallel}, p_e, p_i\}$ in the presence of the global driving parameters (ion temperature gradient dT_{i0}/dx , i.e., pressure gradient dp_{i0}/dx , magnetic field gradient $d|B_0|/dx$, and the inhomogeneous global radial electric field dE_{r0}/dx) describes turbulence caused by the ITG mode and CDIM.

The dynamical equations of fluctuation fields are given in the Appendix after [27]. They are symbolically written as

$$\frac{\partial}{\partial t} f + \mathcal{L}^{(0)} f = \mathcal{N}(f, f) + \tilde{S}_{th}, \quad (1)$$

where f denotes the fluctuating field,

$$f = \begin{pmatrix} \phi \\ J_{\parallel} \\ V_{\parallel} \\ p_e \\ p_i \end{pmatrix}, \quad (2)$$

$P_e = (T_{e0}/T_{i0}) p_e$, $\mathcal{L}^{(0)}$ denotes the linear operator,

$$\mathcal{L}^{(0)} = \begin{pmatrix} i\omega_E + ik_y p'_{i0} + \mu_{\perp} k_{\perp}^2 & i\beta_e^{-1} k_{\parallel} k_{\perp}^{-2} & 0 & ik_y \Omega' k_{\perp}^{-2} & ik_y \Omega' k_{\perp}^{-2} \\ i\xi \xi^{-1} k_{\parallel} & \xi^{-1} (i\omega_E + \xi \eta_{\parallel} + \mu_{e,c} k_{\perp}^2) & 0 & -i\xi \xi^{-1} k_{\parallel} & 0 \\ 0 & 0 & i\omega_E + \mu_{\parallel} k_{\perp}^2 & 0 & ik_{\parallel} \\ -ik_y p'_{e0} - ik_y \Omega' & -\beta_e^{-1} k_{\parallel}^2 & 0 & i\omega_E + ik_{\parallel} + ik_y \Omega' + \chi_{e,c} k_{\perp}^2 & 0 \\ -ik_y p'_{i0} & 0 & i\beta_e k_{\parallel} & 0 & i\omega_E + \chi_{e,c} k_{\perp}^2 \end{pmatrix} \quad (3)$$

and $\mathcal{N}(f, f)$ stands for the nonlinear terms

$$\mathcal{N}(f, f) = - \begin{pmatrix} \nabla_{\perp}^{-2} [\phi, \nabla_{\perp}^2 \phi] \\ (1 - \xi \nabla_{\perp}^{-2})^{-1} [\phi, J_{\parallel}] \\ [\phi, V_{\parallel}] \\ [\phi, P_e] \\ [\phi, P_i] \end{pmatrix}. \quad (4)$$

The bracket $[f, g]$ denotes the Poisson bracket,

$$[f, g] = (\nabla f \times \nabla g) \cdot \mathbf{b}, \quad (5)$$

and $\mathbf{b} = \mathbf{B}_0/B_0$ denotes the unit vector in the direction of the magnetic field. In this article, physics variables (e.g., $\{\phi, A_{\parallel}, V_{\parallel}, P_e, P_i\}$, magnetic field B , electric field, length and time) are normalized according to a standard convention. Various choices of normalization are described in detail in [27]. Transport coefficients by the collisional process are expressed by $\mu_{\perp c}$, $\mu_{e, c}$, $\mu_{\parallel c}$, $\chi_{c, e}$, $\chi_{c, i}$ for the shear viscosity, electron viscosity, parallel viscosity of ions, electron thermal diffusivity and ion thermal diffusivity, respectively. The coefficient

$$\omega_E = V_{E \times B, y} k_y \quad (6)$$

is the Doppler shift by global electric field, and the spatially-inhomogeneous part of it affects the evolution of turbulence so long as the condition $V_{E \times B, y}^2 \ll v_{th, i}^2$ holds [5].

Parameters

$$\xi = \rho_i^2 \delta^{-2}, \text{ and } \xi = 1 + \xi k_{\perp}^{-2} \quad (7)$$

show the finite electron inertia effect. Explicit forms and details are given in the Appendix A.

The explicit driving parameters, which are specified by the inhomogeneity of global parameters, are: the pressure gradient dp_0/dx , the average curvature of the magnetic field Ω' , and the inhomogeneous global radial electric field dE_{r0}/dx . The global gradient $p_0^{-1} dp_0/dx$ controls the growth rate of the semi-micro mode, and the product of two inhomogeneities

$$G_0 = \Omega' \frac{dp_0}{dx}, \quad (8)$$

denotes the excitation parameter for CDIM turbulence and the semi-micro instability. When the ion-temperature gradient is a main source of the pressure gradient, it drives the ITG mode turbulence. The third driving parameter dE_{r0}/dx suppresses turbulence [28-32]. (See [1, 5, 33] for review.) These driving parameters are fixed in the evolution of fluctuating fields under the assumption of the time-space scale separation. This is based on the fact that the system size is taken much longer than the characteristic scale length of the semi-micro mode. The typical time for the evolution of the global parameters is considered much longer than the autocorrelation times of the semi-micro and micro modes.

2.2 Scale separation

We consider the situation where two kinds of microscopic fluctuations are simultaneously excited in the presence of the global inhomogeneity of plasma parameters.

Lagrangian nonlinearity term $\mathcal{N}(f, f)$ gives three effects on a test mode f_k which is taken from the turbulent fluctuations. A part of the Lagrangian nonlinearity ($\mathcal{N}(f, f)$ for f_k) is coherent to the test mode. This coherent part is considered to cause the turbulent drag, which is written as $-\Gamma_k f_k$. The second effect is the modification of the driving term, which was not included in I-V. This is generated by the interaction of modes of different scale lengths, and is symbolically written as $\mathcal{D}_k f_k$. (A symbol 'D' stands for 'drive'.) Other incoherent part is considered as a random self noise \tilde{S}_k . In order to describe the turbulent characteristics, we assume that the system has a large number of degrees of freedom and has many positive Lyapunov exponents. This assumption is a basis to treat the incoherent part \tilde{S}_k as a rapidly varying random noise term.

Symbolically, we write

$$\mathcal{N}_k(f, f) = -\Gamma_k f_k + \mathcal{D}_k f_k + \tilde{S}_k . \quad (9)$$

As has been discussed in I-V, a projection operator \mathcal{P} is introduced to divide the nonlinear interactions into the drag and others.

Scale separation is introduced. The scale lengths of two classes are assumed to be different. A projection operator which separates the semi-micro mode and micro mode is introduced. Semi-micro and micro components are selected by operators \mathcal{P}^l and \mathcal{P}^h , respectively:

$$\mathcal{P}^l + \mathcal{P}^h = 1 . \quad (10)$$

The superscripts l and h denote the semi-micro and micro modes, respectively. The scale-separation means that there exists a mode number k_{sep} in Fourier representation so

that the semi-micro mode is in the region of $|k| < k_{sep}$ and the micro mode satisfies $|k| > k_{sep}$. An operator \mathcal{P}^l is the selection of components which satisfy $|k| < k_{sep}$. Figure 1 illustrates the schematic distribution of the symmetry-breaking flows in the wave-number space.

In calculating the nonlinear drag term, fluctuations which have shorter wavelengths are renormalized. Separation of the nonlinear term into semi-micro and micro components are discussed in Appendix B. One writes the nonlinear effects on the semi-micro and micro modes as

$$\mathcal{X}^l(f, f) = -\left(\Gamma_{(l)}^l + \Gamma_{(h)}^l\right)f^l + \tilde{S}_{(l)}^l + \tilde{S}_{(h)}^l \quad (11)$$

and

$$\mathcal{X}^h(f, f) = -\Gamma_{(h)}^h f^h + \mathcal{D}_{(l)}^h f^h + \tilde{S}_{(h)}^h, \quad (12)$$

respectively. In this expression, the subscripts (l) and (h) denote the contributions from semi-micro and micro modes, respectively. Explicit forms of the drag, drive and noise terms are explained in the next subsection.

2.3 Langevin equation

By use of Eqs.(11) and (12), a Langevin equation is derived as

$$\frac{\partial}{\partial t} f + \mathcal{L}f = \tilde{S} + \tilde{S}_{lh}. \quad (13)$$

For semi-micro elements, one has

$$\mathcal{L} = \mathcal{L}^{(0)} + \left(\Gamma_{(l)}^l + \Gamma_{(h)}^l\right), \quad (14)$$

and

$$\tilde{S} = \tilde{S}_{(l)}^l + \tilde{S}_{(h)}^l + \tilde{S}_{lh}. \quad (15)$$

For micro elements, one has

$$\mathcal{L} = \mathcal{L}^{(0)} + \left(\Gamma_{(h)}^h - \mathcal{D}_{(l)}^h\right) \quad (16)$$

and

$$\tilde{S} = \tilde{S}_{(h)}^h + \tilde{S}_{ih} . \quad (17)$$

The renormalized drag (coherent part) is given in a form of the eddy-viscosity type nonlinear transfer rate γ_j . A random-noise part is regarded to have a shorter decorrelation time than γ_j^{-1} according to RCM [34]. The nonlinear drag term is written in an apparent linear term as

$$\mathcal{P} \mathcal{N}(f, f) = \begin{pmatrix} \mu_N \nabla_{\perp}^2 f_1 \\ \mu_{N\parallel} \nabla_{\perp}^2 f_2 \\ \mu_{Ne} \nabla_{\perp}^2 f_3 \\ \chi_{Ne} \nabla_{\perp}^2 f_4 \\ \chi_{Ni} \nabla_{\perp}^2 f_5 \end{pmatrix} = - \begin{pmatrix} \gamma_1 f_1 \\ \gamma_2 f_2 \\ \gamma_3 f_3 \\ \gamma_4 f_4 \\ \gamma_5 f_5 \end{pmatrix} . \quad (18)$$

Notation here follows the convention in [35]. In this article, suffix $i, j = 1 - 5$ denotes the i -th or j -th field. In the following, Fourier transformation is used, and k, p, q describes the wave number of Fourier components. (Suffix k, p, q is omitted if confusion is not caused.)

The operator to the k -th component, \mathcal{L}_k for Eq.(14) or Eq.(16), is the renormalized operator, which includes the renormalized transfer rates of

$$\gamma_{i,k} = - \sum_{\Delta} M_{i,kpq} M_{i,qkp}^* \tau_{i,qkp}^* \left| \tilde{f}_{1,p}^2 \right| . \quad (19)$$

where $\tau_{i,qkp}$ is the triad-interaction time, and summation Δ indicates the constraint $\mathbf{k} + \mathbf{p} + \mathbf{q} = 0$. The explicit form of the nonlinear interaction matrix is given as, *e.g.*,

$$M_{1,kpq} = (\mathbf{p} \times \mathbf{q}) \cdot \mathbf{b} \frac{(p_{\perp}^2 - q_{\perp}^2)}{k_{\perp}^2} , \quad (20a)$$

$$M_{2,kpq} = (1 + \xi k_{\perp}^{-2})^{-1} (\mathbf{p} \times \mathbf{q}) \cdot \mathbf{b} , \quad (20b)$$

$$M_{(3-5),kpq} = (\mathbf{p} \times \mathbf{q}) \cdot \mathbf{b} , \quad (20c)$$

and the triad-interaction time $\tau_{i,qkp}$ satisfies the relation

$$\left(\partial/\partial t + \mathcal{A}(k) + \mathcal{A}(p) + \mathcal{A}(q) \right) (\tau_{i,kpq}) = I , \quad (21)$$

where \mathbf{I} is the unit vector [35].

The driving part in the nonlinear interactions is deduced. A detail of derivation is discussed in the Appendix B, giving

$$\mathcal{D}_l^h = - \begin{pmatrix} i \omega_{E(l)} & 0 & 0 & 0 & 0 \\ i \xi^{-1} \omega_{2(l)} & i \xi^{-1} \omega_{E(l)} & 0 & 0 & 0 \\ i \omega_{3(l)} & 0 & i \omega_{E(l)} & 0 & 0 \\ i \omega_{4(l)} & 0 & 0 & i \omega_{E(l)} & 0 \\ i \omega_{5(l)} & 0 & 0 & 0 & i \omega_{E(l)} \end{pmatrix} \quad (22)$$

where

$$\omega_{E(l)} = k_y \frac{\partial}{\partial x} \tilde{\Phi}^l - k_x \frac{\partial}{\partial y} \tilde{\Phi}^l \quad (23)$$

is the Doppler shift owing to the $E \times B$ velocity associated with the semi-micro mode, and

$$\omega_{j(l)} = -k_y \frac{\partial}{\partial x} \tilde{f}_j^l + k_x \frac{\partial}{\partial y} \tilde{f}_j^l \quad (j = 2 - 5) \quad (24)$$

represents the modification of plasma parameters by the semi-micro mode. In calculating the $(1, 1)$ element of Eq.(22), the relation

$$\left| \left[\tilde{\Phi}^h, \nabla_{\perp}^2 \tilde{\Phi}^l \right] \right| \ll \left| \left[\tilde{\Phi}^l, \nabla_{\perp}^2 \tilde{\Phi}^h \right] \right| \quad (25)$$

is used.

The self-noise, $\tilde{S} = (\tilde{S}_1, \tilde{S}_2, \tilde{S}_3, \tilde{S}_4, \tilde{S}_5)^T$, has a much shorter correlation time as is discussed in I-V. The nonlinear-noise term for the k -th component is expressed as

$$\tilde{S}_{i,k} = \mathcal{W}(t) \tilde{g}_{i,k}, \quad (26a)$$

$$\tilde{g}_{i,k} \equiv \sum_{\Delta} M_{i,kpq} \sqrt{\tau_{i,kpq}} \zeta_{1,p} \zeta_{i,q} \quad (26b)$$

where $\tilde{g}_{i,k}$ denotes the magnitude of the nonlinear noise term. The rapidly varying temporal dependence is approximated to be given by the Gaussian white noise term $\mathcal{W}(t)$,

$\langle w(t)w(t') \rangle = \delta(t - t')$. This strong assumption of Gaussian white noise is taken in order to adopt the Markovianization in evaluating the correlation functions. The assumption, that the autocorrelation time of $\tilde{S}_{i,k}$ is much shorter than $\gamma_{i,k}^{-1}$, is sufficient for the following derivation of the analysis.

The term $\xi_{j,p}$ in a random noise Eq.(26b) represents the j -th field of q -component in the nonlinear term \mathcal{N} . Their correlation functions satisfy the average relations of the mode, which we call an Ansatz of equivalence in correlation [15, 35] in the following, as

$$\langle \xi_i \xi_j \rangle = \langle f_i f_j \rangle \quad (27)$$

with

$$\langle \xi_{i,p} \xi_{j,q} \rangle \propto \delta_{pq} \quad (28)$$

where the bracket $\langle \rangle$ indicates the statistical average and δ_{pq} is the Kronecker's delta. The Ansatz of equivalence Eq.(27) holds for both the semi-micro components and micro components, respectively.

The thermal excitation is also assumed to be a Gaussian white noise,

$$\tilde{S}_{th,i} = w(t) \tilde{g}_{th,i} . \quad (29)$$

The statistical independence between the incoherent parts of thermal and turbulent fluctuations is also imposed, that is,

$$\langle \tilde{S}_{th,i} \tilde{S}_j \rangle = 0 . \quad (30)$$

2.4 A formal solution

Equation (13) can be solved by introducing the projection operator $\mathbf{A}^{(m)}$ for spectral decomposition ($m = 1 - 5$) which is defined by the relation

$$\exp[-\mathcal{A}(t - \tau)] = \sum_{m=1}^5 \mathbf{A}^{(m)} \exp(-\lambda_m(t - \tau)) . \quad (31)$$

In this equation $-\lambda_m$ ($m = 1 - 5$) represents the eigenvalue of the non-normal matrix \mathcal{L} . The eigenvalue is determined by:

$$\det(\lambda \mathbf{I} + \mathcal{L}) = 0 \quad (32)$$

and I is a unit tensor. Eigenvalues λ 's are ordered as

$$\Re\lambda_1 < \Re\lambda_2 < \Re\lambda_3 < \Re\lambda_4 < \Re\lambda_5. \quad (33)$$

The eigenvector of the eigenvalue $-\lambda_1$ corresponds to the least stable branch, the decay time of which is the longest. Others ($m = 2-5$) denote highly-stable branches, which are assumed to decay much faster.

A formal solution of Eq.(13) is given as

$$f(t) = \sum_{m=1}^5 f^{(m)}(t) \quad (34a)$$

and

$$f^{(m)}(t) = \exp(-\lambda_m t) f^{(m)}(0) + \int_0^t \exp(-\lambda_m(t-\tau)) \mathbf{A}^{(m)} \left\{ \tilde{S}(\tau) + \tilde{S}_{th}(\tau) \right\} d\tau. \quad (34b)$$

where $f^{(m)}(0)$ is the projection of the initial value in the eigenmode basis. The rank of projection operator is unity, and $\mathbf{A}^{(m)}$ is rewritten by an outer product of vectors as

$$\mathbf{A}^{(m)} = \mathbf{V}_L^{(m)} \mathbf{V}_R^{(m)T}. \quad (35)$$

where $\mathbf{V}_L^{(m)}$ and $\mathbf{V}_R^{(m)}$ are vectors of 5 elements. We here choose a normalization

$$V_{L,1}^{(m)} = A_{1,1}^{(m)} \text{ and } V_{R,1}^{(m)} = 1 \quad (36)$$

after the convention in V. (Explicit forms of $\mathbf{A}^{(m)}$ are given in V for three and four field models.) The m -th eigenmode could be selectively calculated as

$$f^{(m)}(t) = \exp(-\lambda_m t) f^{(m)}(0) + \mathbf{V}_L^{(m)} \int_0^t \exp(-\lambda_m(t-\tau)) \mathcal{S}^{(m)}(\tau) d\tau \quad (37)$$

where the projected amplitude of noise source is introduced as

$$\mathcal{S}^{(m)}(\tau) = \mathbf{V}_R^{(m)} \cdot \left\{ \tilde{S}(\tau) + \tilde{S}_{th}(\tau) \right\} \quad (38)$$

The right hand side of Eq.(38) represents the inner-product.

2.5 Statistical average and extended fluctuation dissipation theorem

The long time average of the decomposed amplitude is obtained from Eq.(37). An extended fluctuation dissipation theorem could be derived for the decomposed amplitude. The autocorrelation function of the $i = 1$ element (i.e., the electrostatic potential fluctuation) is given as

$$\langle f_i^{(m)*} f_i^{(m)} \rangle = \frac{1}{2\Re(\lambda_m)} |A_{11}^{(m)}|^2 \langle S^{(m)*} S^{(m)} \rangle. \quad (39)$$

A statistical average is defined as

$$\langle f^* f \rangle \equiv \lim_{t \rightarrow \infty} \frac{1}{t} \int_0^t d\tau f^*(\tau) f(\tau). \quad (40)$$

From Eq.(37), relations between various correlation functions are deduced as

$$\langle f_i^{(m)*} f_j^{(m)} \rangle = \frac{\Re(V_{L,i}^{(m)*} V_{L,j}^{(m)})}{|A_{11}^{(m)}|^2} \langle f_1^{(m)*} f_1^{(m)} \rangle. \quad (41)$$

Combining Eqs.(39) and (41), other autocorrelation functions and cross-correlation functions are given as

$$\langle f_i^{(m)*} f_j^{(m)} \rangle = \frac{\Re(V_{L,i}^{(m)*} V_{L,j}^{(m)})}{2\Re(\lambda_m)} \langle S^{(m)*} S^{(m)} \rangle. \quad (42)$$

For the transparency of the argument, one can take the limit where the amplitude of highly damped branches is neglected,

$$\langle f_i^{(m)*} f_i^{(m)} \rangle \rightarrow 0 \text{ for } (m = 2 - 5). \quad (43)$$

This means that only one pole $m = 1$ is excited for each mode number range (both micro-mode and semi-micro mode). The wave-number ranges of micro-mode and semi-micro mode are separated as is illustrated in Fig.1. In the following, the spectral function of the least stable branches

$$I_{i,k}^{(1)} \equiv \langle f_{i,k}^{(1)*} f_{i,k}^{(1)} \rangle \quad (44)$$

is analyzed with the approximation $\langle f_{i,k}^{(m)*} f_{i,k}^{(m)} \rangle \rightarrow 0$. Therefore we suppress the superscript (1) that denotes the least-stable branch of oscillations. The suffix 1 for λ , which denotes the least stable branch, is also suppressed.

Expressions of the noise sources, Eqs.(15) and (17), are substituted into Eq.(38), and projected elements $S_{(l),k}^l$, $S_{(h),k}^l$, $S_{ih,k}^l$, $S_{(h),k}^h$ and $S_{ih,k}^h$ are calculated accordingly.

One has

$$S_k^l = S_{(l),k}^l + S_{(h),k}^l + S_{ih,k}^l \quad (45)$$

for semi-micro mode and

$$S_k^h = S_{(h),k}^h + S_{ih,k}^h \quad (46)$$

for micro mode, respectively. Noting the statistical independence between noise sources, Eq.(39) is rewritten for semi-micro mode as

$$I_{i,k}^l \equiv \langle f_{i,k}^{l*} f_{i,k}^l \rangle = \frac{1}{2\Re(\lambda^l)} |A_{11}^l|^2 \left(\langle S_{(l),k}^{l*} S_{(l),k}^l \rangle + \langle S_{(h),k}^{l*} S_{(h),k}^l \rangle + \langle S_{ih,k}^{l*} S_{ih,k}^l \rangle \right) \quad (47)$$

and for micro-mode as

$$I_{i,k}^h \equiv \langle f_{i,k}^{h*} f_{i,k}^h \rangle = \frac{1}{2\Re(\lambda^h)} |A_{11}^h|^2 \left(\langle S_{(h),k}^{h*} S_{(h),k}^h \rangle + \langle S_{ih,k}^{h*} S_{ih,k}^h \rangle \right). \quad (48)$$

Equations (47) and (48) give the relations between the fluctuation level $I_{i,k}$ and the noise source. In this sense, they form an extended fluctuation dissipation theorem of the second kind for strongly turbulent plasmas.

The decorrelation rates (inverse of autocorrelation times) for the semi-micro mode and micro mode, λ^l and λ^h in Eqs.(47) and (48), must satisfy the nonlinear dispersion relation Eq.(32). It is written for the semi-micro and micro modes as

$$\det(\lambda^l I + \mathcal{L}^{(0)} + \Gamma_{(l)}^l + \Gamma_{(h)}^l) = 0, \quad (49)$$

and

$$\det\left(\lambda^h I + \mathcal{L}^{(0)} + \Gamma_{(h)}^h - \mathcal{D}_{(l)}^h\right) = 0, \quad (50)$$

respectively. Equations (47)-(50) together with the renormalized forms (19)-(21) form the closed set of equations that determines the statistical averages self-consistently.

2.6 Estimate of eddy damping rate

The renormalization of background fluctuations gives the drag coefficient $\gamma_{i,k}$ of Eq.(19) together with the triad-interaction time $\tau_{i,kpq}$. Under the Markovianization approximation, the triad interaction time is estimated from Eq.(21) as

$$\tau_{i,kpq} \simeq \frac{1}{\gamma_{i,k}} \quad (51)$$

if (k, p) belong to the same class of either semi-micro (l) mode or micro (h) mode or thermal fluctuations. (Here k for the test mode, and p for the back-ground mode.) In Eq.(51), $\gamma_{i,k}$ for micro mode is a sum of the eddy damping rate and damping rate by the thermodynamical dissipation as

$$\gamma_{i,k} = \gamma_{i,k} + \gamma_{ic,k} \quad (52)$$

where γ_c denotes the decorrelation owing to the collisional transport coefficients. It was given in I-V for viscous damping rate as

$$\gamma_{1,k} = \gamma_{1,k} + \gamma_{vc} = \gamma_{1,k} + \mu_c k_{\perp}^2, \quad (53)$$

where μ_c is the molecular viscosity for perpendicular ion motion, being caused by the thermal fluctuations. Other components, e.g., for the parallel current and pressure perturbation, were also given by use of the collisional electron viscosity and collisional thermal diffusivity. $\gamma_{1,k}$ is also written as $\gamma_{v,k}$, illustrating the eddy viscosity damping rate.

With the help of this Markovianization approximation, Eq.(51), the renormalized eddy damping rate in Eq.(19) is approximated as

$$\gamma_{i,k} = - \sum_p M_{i,kpq} M_{i,qkp}^* \gamma_{i,k}^{-1} \left| \tilde{f}_{1,p}^2 \right|, \quad (54a)$$

or

$$\gamma_{i,k} \gamma_{i,k}^* = - \sum_p M_{i,kpq} M_{i,qkp}^* \left| \tilde{f}_{1,p}^2 \right|, \quad (54b)$$

if (k, p) belong to the same class of mode.

If the decorrelation rate of the beat mode (denoted by p) is much larger than that of the test mode, $\gamma_{i,p} \gg \gamma_{i,k}$, one has an estimate

$$\tau_{i,kpq} \approx \frac{1}{\gamma_{i,p}}. \quad (55)$$

When the test mode is chosen from the semi-micro mode, it could also be generated by the beat of rapidly-decaying micro mode, and one has

$$\gamma_{i,k} = - \sum_p^{semi-micro} M_{i,kpq} M_{i,qkp}^* \gamma_{i,k}^{*-1} \left| \tilde{f}_{1,p}^2 \right| - \sum_p^{micro} M_{i,kpq} M_{i,qkp}^* \gamma_{i,p}^{*-1} \left| \tilde{f}_{1,p}^2 \right|. \quad (56)$$

2.6.1 Micro mode

The renormalized damping for microscopic mode is induced by the micro mode, and the right hand side of Eq.(54) is contributed by micro mode as

$$\gamma_{i,k}^h \gamma_{i,k}^{h*} = - \sum_{k'}^{micro\ modes} M_{i,kk'q} M_{i,qkk'}^* \left| \tilde{f}_{1,k'}^2 \right|, \quad (57)$$

where

$$\gamma_{i,k}^h = \gamma_{i,k}^h + \gamma_{ic,k}. \quad (58)$$

Combining Eqs.(57) and (58), one has the relation for microscopic mode as

$$\gamma_{i,k}^h (\gamma_{i,k}^{h*} + \gamma_{ic,k}) = - \sum_{k'}^{micro\ modes} M_{i,kk'q} M_{i,qkk'}^* \left| \tilde{f}_{1,k'}^2 \right|. \quad (59)$$

2.6.2 Semi-micro mode

For the semi-micro mode, both the semi-micro mode and micro mode contribute to the right hand side of Eq.(56), which is rewritten as

$$\gamma_{i,k}^l = \gamma_{(l)i,k}^l + \gamma_{(h)i,k}^l, \quad (60)$$

where

$$\gamma_{(l) i, k}^l = - \sum_p^{semi-micro\ modes} M_{i, kpq} M_{i, qkp}^* \gamma_{i, k}^{*-1} \left| \tilde{f}_{1,p}^2 \right|, \quad (61a)$$

and

$$\gamma_{(h) i, k}^l = - \sum_p^{micro\ modes} M_{i, kpq} M_{i, qkp}^* \gamma_{i, p}^{*-1} \left| \tilde{f}_{1,p}^2 \right|. \quad (61b)$$

The subscripts (l) and (h) denote the contribution from semi-micro mode and micro mode, respectively. Equation (56) is rewritten as

$$\begin{aligned} \gamma_{i, k}^l (\gamma_{i, k}^{l*} + \gamma_{ci, k}) = & - \sum_k^{semi-micro\ modes} M_{i, kk'q} M_{i, qkk'}^* \left| \tilde{f}_{1,k'}^2 \right| \\ & - \sum_{k'}^{micro\ modes} M_{i, kk'q} M_{i, qkk'}^* \frac{\gamma_{i, k}^{l*}}{\gamma_{i, k'}^{h*}} \left| \tilde{f}_{1,k'}^2 \right|. \end{aligned} \quad (62)$$

2.7 Estimate of noise amplitude

2.7.1 Micro mode

The magnitude of source is also evaluated. As in the case of I-V, the self noise source is induced by the micro mode, so that the correlation function $\langle S_{(h), k}^{h*} S_{(h), k}^h \rangle$ is evaluated in the same manner. The explicit procedure is shown in V and is not reproduced here. A diagonalization approximation

$$\sum_{\Delta} \left(2M M^T \tau \langle f_{1,p}^* f_{1,p} \rangle \langle f_{j,q}^* f_{j',q} \rangle \right) \rightarrow C_0^h \gamma_v \langle f_{j,k}^* f_{j',k} \rangle \quad (63)$$

where C_0^h is a numerical constant of order unity, $0 < C_0^h < 1$. (See III for explicit form of coefficient C_0 .) By the help of this approximation, the self-noise term is evaluated.

After the same procedure in V, one has the amplitude of self-induced noise as

$$\langle S_{(h), k}^{h*} S_{(h), k}^h \rangle = C_0^h \gamma_v^h \left| A_{11}^h \right|^{-2} \left| \text{Tr} \mathbf{A}^h \right|^2 I_{1,k}^h, \quad (64)$$

and the total noise amplitude as

$$\langle S_k^{h*} S_k^h \rangle = C_0^h \gamma_{v,k}^h |A_{11}^h|^{-2} |\text{Tr} \mathbf{A}^h|^2 I_{1,k}^h + \text{thermodynamical excitations} . \quad (65)$$

Contribution from thermodynamical excitation is determined by the fluctuation-dissipation theorem for thermodynamical equilibrium. An explicit form is given in II and is not repeated here.

2.7.2 Semi-micro mode

The self noise source is induced by the micro mode as well as semi-micro mode,

$$\langle S_k^{l*} S_k^l \rangle = \langle S_{(l),k}^{l*} S_{(l),k}^l \rangle + \langle S_{(h),k}^{l*} S_{(h),k}^l \rangle + \text{thermodynamical excitations} . \quad (66)$$

The correlation function $\langle S_{(l),k}^{l*} S_{(l),k}^l \rangle$, which is induced by the semi-micro mode, is evaluated in a same manner as for the micro mode. A diagonalization approximation Eq.(63) is also used for the semi-micro mode

$$\sum_{\Delta}^{\text{semi-micro modes}} \left(2M M \tau \langle f_{1,p}^{*} f_{1,p} \rangle \langle f_{j,q}^{*} f_{j',q} \rangle \right) \rightarrow C_0^l \gamma_v^l \langle f_{j,k}^{l*} f_{j',k}^l \rangle \quad (67)$$

and the amplitude of self-induced part of the nonlinear noise is given as

$$\langle S_{(l)}^{l*} S_{(l)}^l \rangle = C_0^l \gamma_v^l |A_{11}^l|^{-2} |\text{Tr} \mathbf{A}^l|^2 I_{1,k}^l \quad (68)$$

for the semi-micro mode. The correlation function $\langle S_{(h),k}^{l*} S_{(h),k}^l \rangle$ is given by summations like

$$\sum_{\Delta}^{\text{micro modes}} \left(2M M \tau \langle f_{1,p}^{h*} f_{1,p}^h \rangle \langle f_{j,q}^{h*} f_{j',q}^h \rangle \right) . \quad (69)$$

In this summation, wave numbers (p, q) belong to those of micro mode, but their beat $p + q$ belongs to the semi-micro mode. Magnitude of $M M$ is reduced, relatively, by the factor of $(k/k^h)^2$ (k is the mode number of the test mode (semi-micro mode), and k^h is that of micro mode). By noting this fact, one possible estimate of Eq.(69) is

$$\sum_{\Delta}^{\text{micro modes}} \left(2M M \langle f_{1,p}^{h*} f_{1,p}^h \rangle \langle f_{j,q}^{h*} f_{j',q}^h \rangle \right) \rightarrow \left(\frac{k}{k^h} \right)^2 \hat{C}_0^h \gamma_v^h \langle f_{j,k}^{h*} f_{j',k^h}^h \rangle , \quad (70)$$

where \hat{C}_0^h is a numerical constant of the order of C_0^h . Using the typical mode number of micro mode k_0^h , one has

$$\sum_{\Delta}^{micro\ modes} \left(2M M \langle f_{1,p}^{h*} f_{1,p}^h \rangle \langle f_{j,q}^{h*} f_{j,q}^h \rangle \right) \rightarrow \frac{k^2}{(k_0^h)^4} \hat{C}_0^h \gamma_v^h I_j^h, \quad (71)$$

where

$$I_j^h = \sum_k I_{j,k}^h = \sum_k \langle f_{j,k}^{h*} f_{j,k}^h \rangle \quad (72)$$

is the total fluctuation amplitude for the j-th field of micro mode.

The nonlinear noise for semi-micro mode, which is driven by micro mode, is evaluated as

$$\langle S_{(h)}^* S_{(h)} \rangle = \hat{C}_0^h \gamma_v^h \frac{k^2}{(k_0^h)^4} |A_{11}^l|^{-2} |\text{Tr} \mathbf{A}^l|^2 I_1^h. \quad (73)$$

The total noise amplitude for semi-micro mode is given by combining Eqs.(68) and (73), and is expressed as

$$\begin{aligned} \langle S_k^* S_k \rangle = & |A_{11}^l|^{-2} |\text{Tr} \mathbf{A}^l|^2 \left(C_0^l \gamma_v^l I_{1,k}^l + \hat{C}_0^h \gamma_v^h \frac{k^2}{(k_0^h)^4} I_1^h \right) \\ & + \text{thermodynamical excitations}. \end{aligned} \quad (74)$$

2.8 Estimate of fluctuation dissipation relation

Estimate of noise source term is combined with the extended fluctuation dissipation theorem, Eqs.(47) and (48). The fluctuation level is determined in a self-consistent manner.

2.8.1 Micro mode

Equation (65) is substituted in Eq.(48), and the noise source term is eliminated from Eq.(48). One has

$$I_{1,k}^h = \frac{C_0^h \gamma_{v,k}^h}{2\Re(\lambda^h)} I_{1,k}^h + \text{thermal fluctuations}. \quad (75)$$

In deriving Eq.(75), the relation

$$\text{Tr} \mathbf{A}^h = 1 \quad (76)$$

is used. The expression of the thermal fluctuations in Eq.(75) has been given in II.

2.8.2 Semi-micro mode

For the semi-micro mode, Eq.(74) is substituted into Eq.(47). The similar procedure is employed, $\text{Tr} \mathbf{A}^l = 1$, and one has

$$I_{1,k}^l = \frac{1}{2\Re(\lambda^l)} \left(C_0^l \gamma_v^l I_{1,k}^l + \hat{C}_0^h \gamma_v^h \frac{k^2}{(k_0^h)^4} I_1^h \right) + \text{thermal fluctuations} . \quad (77)$$

2.9 Strong turbulence limit

The phase diagram of the turbulent fluctuations and thermodynamical fluctuations are given in I-IV. The case of strong turbulence limit is adopted, which is relevant for inhomogeneous and confined plasmas. The thermodynamical fluctuations are neglected in Eqs.(75) and (77). For nontrivial solutions of fluctuations, we have

$$\Re(\lambda^h) = \frac{C_0^h}{2} \gamma_v^h , \quad (\text{or } I_{1,k}^h = 0) \quad (78)$$

and

$$\Re(\lambda^l) I_{1,k}^l = \frac{C_0^l}{2} \gamma_v^l I_{1,k}^l + \frac{\hat{C}_0^h}{2} \gamma_v^h \frac{k^2}{(k_0^h)^4} I_1^h . \quad (79)$$

The nonlinear dispersion relation Eqs.(49) and (50), the renormalization relation Eqs.(59) and (62), and the fluctuation dissipation theorems Eqs.(78) and (79) form a set of equations that determines the fluctuation level and autocorrelation time self-consistently.

2.10 Average model

Spectrum averages appear in renormalization relations and extended fluctuation dissipation theorems. Order of magnitude estimate which is based on dimensional arguments is made assuming that summations converge. Discussion is made in Appendix C.

An order of magnitude estimate of Eq. (59) is given as

$$\gamma_i^h(\gamma_i^{h*} + \gamma_{ic}^h) \approx (k_0^h)^4 I_i^h, \quad (80)$$

where γ_i^h is the characteristic eddy-damping rate of the micro mode, I_j^h is the total fluctuation amplitude for the j -th field of micro-mode Eq.(72), and k_0^h is the characteristic wave number of the micro mode. Equation (62) is evaluated as

$$\gamma_i^l(\gamma_i^{l*} + \gamma_{ic}^l) \approx (k_0^l)^4 I_i^l + (k_0^l)^2 (k_0^h)^2 \frac{\gamma_i^{l*} + \gamma_{ic}^l}{\gamma_i^{h*} + \gamma_{ic}^h} I_i^h, \quad (81)$$

where the total fluctuation level for the j -th field of semi-micro mode is given by

$$I_j^l = \sum_k I_{j,k}^l = \sum_k \langle f_{j,k}^{l*} f_{j,k}^l \rangle. \quad (82)$$

and γ_i^l is the characteristic eddy-damping time of the semi-micro mode, and k_0^l is the characteristic wave number of the semi-micro mode.

Extended fluctuation-dissipation theorem for the semi-micro mode Eq.(79) is approximated as

$$\Re e(\lambda^l) I_1^l = \frac{C_0^l}{2} \gamma_v^l I_1^l + \frac{\hat{C}_0^h}{2} \gamma_v^h \left(\frac{k_0^l}{k_0^h} \right)^4 I_1^h \quad (83)$$

where λ^l is the characteristic (spectrum-averaged) eigenvalue of the nonlinear dispersion relation.

With these simplifications, the solutions of nonlinear dispersion relation (49) and (50), together with renormalization relation Eqs. (80), (81) and extended FDT Eqs. (78) and (83), determine the fluctuation level and correlation functions self-consistently. Solutions of the nonlinear eigen values λ^l and λ^h are discussed in the next section.

2.11 Turbulence-driven transport

2.11.1 Test particle diffusion

Transport of test particle is calculated by use of the spectral functions of the fluctuating fields. The velocity of the test particles in the x -direction by the k -component of the fluctuation field, $V_{x,k}(t)$, is given as $V_{x,k}(t) = ik_y f_{1,k}(t)$. The displacement in the direction of the global gradient, x -direction, is given as

$$x(t) - x(0) = -i \sum_k k_y \int_0^t d\tau f_{1,k}(\tau). \quad (84)$$

Substituting Eq.(37) into Eq.(84), the statistical average of the mean deviation is obtained. Explicit calculation is presented in V as

$$\left\langle \left| x(t) - x(0) \right|^2 \right\rangle = \sum_k k_y^2 A_{1l}^{(1)2} \frac{1}{(\Re \lambda)^2} \left\langle S_k^{(1)*} S_k^{(1)} \right\rangle \int_0^t d\tau, \quad (85)$$

giving the test particle diffusion coefficient D_{test} in terms of the noise source as

$$D_{test} = \lim_{t \rightarrow \infty} \frac{1}{t} \left\langle \left| x(t) - x(0) \right|^2 \right\rangle = \sum_k k_y^2 A_{1l}^{(1)2} \frac{1}{(\Re \lambda)^2} \left\langle S_k^{(1)*} S_k^{(1)} \right\rangle. \quad (86)$$

By use of Eq.(39), it is rewritten in terms of fluctuation spectrum as

$$D_{test} = \sum_k \frac{2k_y^2}{\Im e \lambda} I_{1,k}. \quad (87)$$

Both the semi-micro and micro modes contribute to the test particle diffusion coefficient. Using the average model of §2.10, the test particle diffusion coefficient is estimated as

$$D_{test} = \frac{(k_0^l)^2}{\Re e \lambda^l} I_1^l + \frac{(k_0^h)^2}{\Re e \lambda^h} I_1^h. \quad (88)$$

2.11.2 Cross-field flux of energy

Cross field transport of energy is obtained by calculating the cross-correlation functions. The ion energy flux which is induced by the turbulent $E \times B$ motion is given as

$$q_{i0,x} = - \left\langle p_i^* \frac{\partial}{\partial y} \phi \right\rangle. \quad (89)$$

This quantity is calculated by use of the cross-correlation function

$$q_{i0,x} = - \Im m \sum_k k_y \left\langle f_{5,k}^* f_{1,k} \right\rangle. \quad (90)$$

By use of Eq.(41), the cross field heat flux is given by the autocorrelation function for the fluctuating potential as

$$q_{i0,x} = - \sum_k \frac{k_y \Im m(V_{L,5}^* V_{L,1})}{|A_{1,1}|^2} I_{1,k}. \quad (91)$$

In the framework of the average model, we have an evaluation as

$$q_{i0,x} = -\Im m \left(k_{0,y}^l V_{L,5}^* V_{L,l} |A_{l,l}|^{-2} \right)^l I_l^l - \Im m \left(k_{0,y}^h V_{L,5}^* V_{L,l} |A_{l,l}|^{-2} \right)^h I_l^h. \quad (92)$$

3. Three Field Modelling

The decomposition Eq.(31) for the five-field model is in principle possible; nevertheless it is often very tedious. It sometimes is more physically transparent to use a truncated form of the renormalized dielectric tensor \mathcal{L} . A simple truncated model of \mathcal{L} is introduced, and analytic solutions for the nonlinear dispersion relation are investigated in the following.

3.1 Renormalized dielectric tensor and eigenvalue

3.1.1 Semi-micro mode

To obtain a three field model, firstly the electron inertia effect is neglected in the Ohm's law, and the electrostatic limit is assumed, i.e., the inductive term in the Ohm's law is neglected. Then the system turns to be the dynamical equations of four variables $\{\phi, V_{\parallel}, n, p_i\}$. In addition to it, often employed is the approximation that the Boltzmann relation for the electron response, $\tilde{n} = \tilde{\phi}$ or the low-electron temperature limit holds as

$$\tilde{p}_e \rightarrow 0 \text{ for } T_e \ll T_i. \quad (93)$$

If one keeps the current perturbation, the influence of parallel resistivity on the semi-micro mode can be studied. The resistivity can enhance the growth rate, so that the enhancement of anomalous resistivity by micro mode can increase the turbulence level of the semi-micro mode. However, this influence on the growth rate is small in the range of parameters of interest [27]. Therefore this influence is not kept in this article.

With this simplification, $A_{\parallel} \rightarrow 0$ and $\tilde{p}_e \rightarrow 0$, the reduced set of equations is composed of three equations for the variables of

$$f^l = \begin{pmatrix} \phi \\ V_{\parallel} \\ p_i \end{pmatrix} \quad (94)$$

as

$$\mathcal{L}^{(0)} = \begin{pmatrix} i\omega_{E1} + ik_y p'_{i0} + \mu_{\perp} k_{\perp}^2 & 0 & ik_y \Omega' k_{\perp}^{-2} \\ 0 & i\omega_{E1} + \mu_{\parallel} k_{\parallel}^2 & ik_{\parallel} \\ -ik_y p'_{i0} & i\beta k_{\parallel} & i\omega_{E1} + \chi_{i,c} k_{\perp}^2 \end{pmatrix}. \quad (95)$$

The renormalized operator \mathcal{L}^l for the semi-micro mode is given as

$$\mathcal{L}^l = \begin{pmatrix} i\omega_{E1} + ik_y p'_{i0} + \Upsilon_v^l & 0 & ik_y \Omega' k_{\perp}^{-2} \\ 0 & i\omega_{E1} + \Upsilon_{\parallel}^l & ik_{\parallel} \\ -ik_y p'_{i0} & i\beta k_{\parallel} & i\omega_{E1} + \Upsilon_p^l \end{pmatrix}. \quad (96)$$

In this equation,

$$\omega_{E1} = \frac{1}{B} \frac{d}{dr} E_r \quad (97)$$

represents the shearing rate of $E \times B$ flow by the global radial electric field. Quantities Υ_v^l , Υ_{\parallel}^l and Υ_p^l are the sum of eddy damping rate and collisional damping rate, owing to the shear viscosity of perpendicular ion motion, the shear viscosity of parallel ion motion and the ion thermal diffusivity, respectively. The drag terms are expressed as

$$\Gamma_k^l = \begin{pmatrix} \mu_N \nabla_{\perp}^2 \tilde{\Phi}_k^l \\ \mu_{N\parallel} \nabla_{\perp}^2 \tilde{V}_{\parallel,k}^l \\ \chi_{Ni} \nabla_{\perp}^2 \tilde{P}_{i,k}^l \end{pmatrix} = - \begin{pmatrix} \gamma_v^l \tilde{\Phi}_k^l \\ \gamma_{\parallel}^l \tilde{V}_{\parallel,k}^l \\ \gamma_p^l \tilde{P}_{i,k}^l \end{pmatrix}. \quad (98)$$

The drag term is given as a sum of those induced by the semi-micro mode and those by micro mode as,

$$\Gamma_k^l = \Gamma_{(l)k}^l + \Gamma_{(h)k}^l \quad (99)$$

where

$$\Gamma_{\{h\}k}^l = - \begin{pmatrix} \gamma_{\{h\}v}^l \tilde{\Phi}_k^l \\ \gamma_{\{h\}\parallel}^l \tilde{V}_{\parallel,k}^l \\ \gamma_{\{h\}p}^l \tilde{P}_{i,k}^l \end{pmatrix} \quad (100a)$$

and

$$\Gamma_{\{l\}k}^l = - \begin{pmatrix} \gamma_{\{l\}v}^l \tilde{\Phi}_k^l \\ \gamma_{\{l\}\parallel}^l \tilde{V}_{\parallel,k}^l \\ \gamma_{\{l\}p}^l \tilde{P}_{i,k}^l \end{pmatrix}. \quad (100b)$$

(Correspondences between γ^l 's in §2 are $\gamma_v^l = \gamma_1^l$, $\gamma_{\parallel}^l = \gamma_3^l$ and $\gamma_p^l = \gamma_5^l$. Because the number of variables, being denoted by i, j , is different in §2 and §3, we use the symbols v, \parallel , and p for the suffix here.) Renormalization of background fluctuations of semi-micro mode gives $\Gamma_{\{l\}k}^l$, and the one of micro mode yields $\Gamma_{\{h\}k}^l$.

This set of equations describes the (resistive) ITG-mode in the presence of the magnetic field inhomogeneity. The coupling between the ITG mode and the interchange mode could be investigated. The influence of micro mode turbulence on the renormalized operator \mathcal{L}^l is included through the nonlinear eddy damping rates γ_v^l , γ_{\parallel}^l and γ_p^l , as is shown by Eq.(100a).

Nonlinear eigenvalue equation Eq.(32) is solved by adopting the expression Eq.(96). The local dispersion relation in the absence of the electric field shear is given

$$\hat{\lambda}^3 + i\omega_* \hat{\lambda}^2 + \left(k_y^2 k_{\perp}^{-2} p_{i0}' \Omega' + \beta k_{\parallel}^2 \right) \hat{\lambda} + i\omega_* \beta k_{\parallel}^2 = 0, \quad (101)$$

with

$$\hat{\lambda}^l = \lambda^l - \gamma_v^l. \quad (102)$$

In deriving Eq.(101), a relation

$$\gamma_v^l \simeq \gamma_{\parallel}^l \simeq \gamma_p^l \quad (103)$$

is used for the transparency of the analysis. The approximation, Eq.(103), means that the turbulent Prandtl number is close to unity $P_r^{turb} \equiv \mu \sqrt{\chi_{pi}} \simeq 1$. The quantitative study, in which the turbulent Prandtl number is determined self-consistently, has shown that the

approximation $P_r^{turb} \simeq 1$ is a relevant approximation for usual situations. Nonlocal solution in the presence of the magnetic shear has been discussed in literature. (See, e.g., [2, 27, 36].) If the magnetic shear is not strong, the nonlocal solution of Eqs.(32) and (96) is the ITG mode coupled with interchange mode (or magnetic curvature driven ITG mode), and belongs to the family to which the toroidal ITG mode belongs. In the strong shear case, the eigenvalue has been obtained for the long-wave length ITG mode (which might not be the fastest-growing, but is important for the turbulent-driven transport) is given as [2, 36]

$$\Re \hat{\lambda} = -\frac{r}{qR} s (1 + \eta_i) \left| \omega_{*i} \right|. \quad (104)$$

where ω_{*i} is the ion drift frequency. In the weak shear limit, one has the magnetic-curvature driven ITG mode as [27]

$$\hat{\lambda} = \frac{1}{2} \left(-i - \sqrt{\Omega' (1 + \eta_i)} \right) \left| \omega_{*i} \right|. \quad (105)$$

Note that the minus sign of the real part of the eigen value λ indicates the instability. By taking the case of Eq.(104), one has the form of the eigenvalue for the semi-micro mode as

$$\Re \lambda^l = -\gamma_0^l + \gamma_v^l, \quad (106)$$

where

$$\gamma_0^l = \frac{r}{qR} s (1 + \eta_i) \left| \omega_{*i} \right|. \quad (107)$$

(Order of magnitude of $\left| \omega_{*i} \right|$ is given by $\left| \omega_{*i} \right| \sim O(v_{thi}/a)$ for $k\rho_i \sim 1$ in a dimensional form.)

In the presence of the inhomogeneous radial electric field, the ω_{E1} term in Eq.(96) affects the eigenvalue. In the plasma frame, the anti-symmetric part of ω_{E1} with respect to the change of $x \rightarrow -x$ has the important contribution. The nonlocal analysis has been performed, showing that the eigenvalue γ_0^l is modified. Explicit form has been discussed in literature. One characteristic feature is that the growth rate of the mode is strongly suppressed when ω_{E1} reaches a critical value ω_{Ec}^l . The critical value ω_{Ec}^l is given as [36]

$$\omega_{Ec}^l = \frac{2}{\sqrt{1+\eta_i}} \gamma_0^l \quad (108)$$

Choosing a fitting function to be the Lorentzian form, the growth rate is modelled as

$$\gamma_{0E}^l = \frac{\gamma_0^l}{1 + (\omega_{E1}/\omega_{Ec}^l)^2} \quad (109)$$

We have the nonlinear eigenvalue for the semi-micro mode as

$$\Re \lambda^l = - \frac{\gamma_0^l}{1 + (\omega_{E1}/\omega_{Ec}^l)^2} + \gamma_v^l \quad (110)$$

3.1.2 Micro mode

For the microscopic mode, we study the current-diffusive (or resistive) interchange mode, and take a simplification

$$\tilde{V}_{\parallel} \rightarrow 0 \quad (111)$$

together with Eq.(93). The extension to the case of finite electron pressure perturbation is straightforward, and has been discussed in [37, 38]. In the limit of Eqs.(93) and (111), the reduced system is obtained with variables

$$\mathbf{f}^h = \begin{pmatrix} \tilde{\Phi} \\ \tilde{J}_{\parallel} \\ \tilde{p}_i \end{pmatrix} \quad (112)$$

For this set of variables, the linear operator and the nonlinear drag term are reduced to

$$\mathcal{L}^h(0) = \begin{pmatrix} i \omega_{E1} + i k_y p'_{i0} + \mu_{\perp c} k_{\perp}^2 & i \beta_e^{-1} k_{\parallel} k_{\perp}^{-2} & i k_y \Omega' k_{\perp}^{-2} \\ i \xi \xi^{-1} k_{\parallel} & \xi^{-1} (i \omega_{E1} + \mu_{e,c} k_{\perp}^2) & 0 \\ -i k_y p'_{i0} & 0 & i \omega_{E1} + \chi_{i,c} k_{\perp}^2 \end{pmatrix} \quad (113)$$

and

$$\Gamma_{(h),k}^h = \mathcal{P} \mathcal{N}(f, f) = \begin{pmatrix} \mu_N^h \nabla_{\perp}^2 \tilde{\Phi}_k^h \\ \mu_{Ne}^h \nabla_{\perp}^2 \tilde{J}_{\parallel}^h \\ \chi_{Ni}^h \nabla_{\perp}^2 \tilde{p}_{i,k}^h \end{pmatrix} = - \begin{pmatrix} \gamma_v^h \tilde{\Phi}_k^h \\ \gamma_e^h \tilde{J}_{\parallel,k}^h \\ \gamma_p^h \tilde{p}_{i,k}^h \end{pmatrix} \quad (114)$$

For the micro mode, we use the symbols v , e , and p for the suffix of eddy damping rates here. (Relations with those in §2 are: $\gamma_v^h = \gamma_1^h$, $\gamma_e^h = \gamma_2^h$ and $\gamma_p^h = \gamma_3^h$.) The eddy damping rate for parallel electron motion (electron viscosity) is close to the thermal diffusivity due to the micro turbulence. We use the suffix e for the electron viscosity. It is noted again that the form of the operator $\mathcal{L}^{(0)}$ is simplified version of the one for the CDIM (CDBM) turbulence. The finite ion gyroradius effect modifies the form of $\mathcal{L}^{(0)}$, influencing the solution of the nonlinear dispersion relation. However, it has been shown that the qualitative feature of CDIM turbulence is not affected much by the finite ion gyroradius effect [38]. Based upon this confirmation, we choose here a simplified form of $\mathcal{L}^{(0)}$.

The operator which renormalizes the background micro turbulence, \mathcal{Z}^h , is given as

$$\mathcal{Z}^h f_k^h \equiv \mathcal{L}^{(0)} f_k^h + \Gamma_{(h),k}^h. \quad (115)$$

Substituting Eqs.(113) and (114) into Eq.(115), the operator \mathcal{Z}^h is given as

$$\mathcal{Z}^h = \begin{pmatrix} i \omega_{E1} + i k_y p'_{i0} + \gamma_v^h & i \beta_e^{-1} k_{\parallel} k_{\perp}^{-2} & i k_y \Omega' k_{\perp}^{-2} \\ i \xi \xi^{-1} k_{\parallel} & \xi^{-1} (i \omega_{E1} + \gamma_e^h) & 0 \\ -i k_y p'_{i0} & 0 & i \omega_{E1} + \gamma_p^h \end{pmatrix} \quad (116)$$

In simplifying Eq.(3) into Eq.(113), the current-diffusive limit $\xi \eta_{\parallel} \ll \mu_e, c k_{\perp}^2$ is taken. The other limit, i.e., resistive limit $\xi \eta_{\parallel} \gg \mu_e, c k_{\perp}^2$, is also taken and similar argument can be developed [39, 40].

The nonlinear drive operator, which is induced by the semi-micro mode, is given for this reduced model as

$$\mathcal{D}_{(l)}^h = - \begin{pmatrix} i \omega_{E(l)} & 0 & 0 \\ i \xi^{-1} \omega_{2(l)} & i \xi^{-1} \omega_{E(l)} & 0 \\ i \omega_{5(l)} & 0 & i \omega_{E(l)} \end{pmatrix}. \quad (117)$$

Therefore the modification of gradient for micro mode by semi-micro mode is kept in electrostatic potential and ion pressure. The current profile modification which is associated with the semi-micro mode is small. The nonlinear drive operator for micro mode is simplified as

$$\mathcal{D}_{(l)}^h = - \begin{pmatrix} i \omega_{E(l)} & 0 & 0 \\ 0 & i \xi^{-1} \omega_{E(l)} & 0 \\ i \omega_{\nabla p(l)} & 0 & i \omega_{E(l)} \end{pmatrix} \quad (118)$$

the influence of the $E \times B$ flow shear $\omega_{E(l)}$ is given by Eq.(23), and the $(3, 1)$ element is given as

$$\omega_{\nabla p(l)} = -k_y \frac{\partial}{\partial x} \tilde{p}_i^l + k_x \frac{\partial}{\partial y} \tilde{p}_i^l. \quad (119)$$

The total renormalized operator is given as

$$\mathcal{L}_k^h = \hat{\mathcal{L}}_k^h - \mathcal{D}_{(l),k}^h. \quad (120)$$

The operator $\hat{\mathcal{L}}^h$ is discussed in the previous publications, and the term $\mathcal{D}_{(l),k}^h$ represents the influence of semi-micro mode on the microscopic turbulence.

The operator $\mathcal{D}_{(l),k}^h$ includes the fluctuating field associated with the semi-micro perturbations. It fluctuates in time. In obtaining the solution of the eigenvalue equation (32) with Eq.(120), two limiting cases are considered.

One limit is the case that the autocorrelation time of the semi-micro mode is much longer than the autocorrelation time of the micro mode. In this case, the value of $\mathcal{D}_{(l),k}^h$ does not change during the autocorrelation time of the micro fluctuations. Therefore, the operator $\mathcal{D}_{(l),k}^h$ is approximated as constant in time in solving the dynamical equation of the microscopic fluctuations. We call this case 'dc-limit'.

The other limit is that the autocorrelation time of the semi-micro mode is much shorter than that of the micro mode. In this case, the operator $\mathcal{D}_{(l),k}^h$ gives rise to a

random oscillation effect on the dynamics of the test mode of micro fluctuations. This case is called 'random oscillator limit'. (See [1].)

As a first step of the analysis, we take the 'dc-limit' here. This is because the correlation time of the semi-micro mode is usually much longer than that of the micro mode, when nonlinear dynamics of each component is analyzed separately. This is the basis to employ the dc-limit in this article. The opposite limit might be more relevant, if one chooses the 'zonal flow' as a semi-micro component. Its autocorrelation time could be equal to or shorter than the micro fluctuations [41]. Such a case requires the statistical method for random oscillators. The statistical approach has been discussed in literature [1, 42].

In the absence of the nonlinear drive term by the semi-micro mode and radial electric field, the eigenvalue λ for the nonlinear dispersion relation has been obtained as [43]

$$\Re \lambda \approx G_0^{1/2} \left(- \left(\frac{\chi}{\chi_0} \right)^{1/5} + \frac{\chi}{\chi_0} \right) \omega_{Ap}, \quad (121)$$

showing that this mode is subcritically excited by the turbulence-driven electron viscosity. In this equation,

$$\gamma_0^h = \sqrt{G_0} \omega_{Ap}. \quad (122a)$$

represents the typical growth rate of the mode, $\omega_{Ap} = v_{Ap}/a$ (v_{Ap} being the poloidal Alfvén velocity), χ/χ_0 is the normalized amplitude of the micro mode fluctuation

$$\chi_0 \equiv \frac{G_0^{3/2}}{s^2} \frac{c^2}{\omega_p^2} \omega_{Ap}, \quad (122b)$$

$$\frac{\chi}{\chi_0} = \frac{T}{eB} \frac{1}{\chi_0} \frac{e\tilde{\Phi}}{T}, \quad (122c)$$

and

$$\hat{k}_0^h = 0.58 (G_0 \chi / \mu)^{1/4} \chi_0^{-1/2} \quad (123)$$

is the characteristic mode number ($G_0 = p'_{i0} \Omega'$ denotes the driving parameter owing to the global inhomogeneities). This branch of oscillations is subject to the subcritical excitation, and subcritical property is discussed in detail in [1, 5]. In this article, we are interested in the interplay between the different turbulent modes, so that a simplified model

form is used. In the vicinity of the zero of the eigenvalue, λ in Eq.(121) is Taylor-expanded and an approximate form is given as

$$\Re \lambda^h = -\gamma_0^h + \gamma_v^h. \quad (124)$$

In the presence of the inhomogeneous radial electric field, the nonlocal analysis has been performed, and the eigenvalue γ_0^h is modified by the Doppler shift as

$$\gamma_{0E}^h = \frac{\gamma_0^h}{1 + (\omega_{E1}/\omega_{Ec}^h)^2}. \quad (125)$$

where

$$\omega_{Ec}^h \approx s \frac{v_{thi}}{\sqrt{aR}} \quad (126)$$

represents the critical value of the inhomogeneous radial electric field for the suppression of the micro turbulence [44]. Taking this effect into account, the nonlinear eigenvalue for the micro mode is modified as

$$\Re \lambda^h = -\frac{\gamma_0^h}{1 + (\omega_{E1}/\omega_{Ec}^h)^2} + \gamma_v^h. \quad (127)$$

Next, the influences of the drive-term by the semi-micro mode are considered. In the presence of the driving terms, the pressure gradient and radial electric field shear are enhanced through the terms $\omega_{\nabla p(l)}$ and $\omega_{E(l)}$, respectively.

Owing to the $\omega_{\nabla p(l)}$ term, the driving source for fluctuations is enhanced. The absolute value of $\omega_{\nabla p(l)}$ is evaluated as

$$|\omega_{\nabla p(l)}| = |k_y^h k_x^l p_l^l| = |k_y^h k_x^l| \sqrt{I_3^l}. \quad (128)$$

(Note that the pressure gradient in the y-direction is induced by the semi-micro mode. However, this gradient is in the perpendicular direction of the gradient of the magnetic field strength, and has little influence on the interchange mode turbulence.) In driving micro mode, the pressure gradient is effectively increased as

$$p'_{i0} \rightarrow p'_{i0} + |k_x^l| \sqrt{I_3^l}. \quad (129)$$

In a region where the pressure gradient is enhanced by the semi-micro mode, the microscopic fluctuations are more strongly excited with Eq.(122a) being replaced by

$$\gamma_0^h \rightarrow \gamma_{(l)}^h{}_{driven} = \sqrt{\left(p_{i0}' + |k_x^l| \sqrt{I_3^l}\right) \Omega'} . \quad (130)$$

The relation between the pressure perturbation and electrostatic potential perturbation is given by Eq.(41). An explicit form for \mathbf{A} is given in V, and the relation between I_3 and I_1 is given as

$$I_3^l = \left| \frac{k_y^l p_0'}{\gamma_p^l - \lambda^l} \right|^2 I_1^l . \quad (131a)$$

A further simplification is often employed as

$$\sqrt{I_3^l} \approx \left| \frac{k_y^l p_0'}{\gamma_v^l} \right| \sqrt{I_1^l} , \quad (131b)$$

giving an expression

$$\gamma_{(l)}^h{}_{driven} \approx \gamma_0^h \sqrt{1 + |k_0^l|^2 / 2 \gamma_v^l} \sqrt{I_1^l} . \quad (131c)$$

The $E \times B$ flow shear effect is also enhanced by the semi-micro fluctuations. In the diagonal term of the renormalized tensor, the new term $\omega_{E(l)}$ appears and replacement

$$\omega_{E1} \rightarrow \omega_{E1} + \omega_{E(l)} \quad (132)$$

holds. The asymmetric part of $\omega_{E(l)}$ influences the turbulence level. Figure 2 illustrates the stretching the flow pattern of the micro mode in the presence of semi-micro mode fluctuations. The semi-micro mode stabilizes the micro mode through the mechanism which is effective in turbulence suppression by the sheared flow. Because the phase of $\omega_{E(l)}$ is statistically independent of that of dc component ω_{E1} , we have

$$\left\langle \left(\omega_{E1} + \omega_{E(l)} \right)^2 \right\rangle = \left(\omega_{E1} \right)^2 + \left\langle \left(\omega_{E(l)} \right)^2 \right\rangle . \quad (133)$$

The replacement

$$(\omega_{E1})^2 \rightarrow (\omega_{E1})^2 + \left\langle (\omega_{E(l)})^2 \right\rangle \quad (134)$$

should be taken into account in Eq.(127) as

$$\Re \lambda^h = - \frac{\gamma_{(l)}^h \text{driven}}{1 + (\omega_{E1}/\omega_{Ec}^h)^2 + \left\langle (\omega_{E(l)}/\omega_{Ec}^h)^2 \right\rangle} + \gamma_v^h. \quad (135)$$

The amplitude of the frequency shift $\omega_{E(l)}$ is in proportion to the amplitude of the electrostatic potential perturbation associated with semi-micro fluctuations. The fluctuation amplitude of the electrostatic potential is given as

$$|\tilde{\phi}| = \sqrt{I_1^l}. \quad (136)$$

Substituting Eq.(136) into Eq.(23), we have the relation

$$|\omega_{E(l)}| = (k^l)^2 \sqrt{I_1^l}. \quad (137)$$

Substituting Eq. (137) into Eq.(135), the influence of the driving nonlinearities $\mathcal{D}_{(l)}^h$ on the eigenvalue of the micro mode is obtained as

$$\Re \lambda^h = - \frac{\gamma_{(l)}^h \text{driven}}{1 + (\omega_{E1}/\omega_{Ec}^h)^2 + (k^l)^4 (\omega_{Ec}^h)^{-2} I_1^l} + \gamma_v^h. \quad (138)$$

3.2 Nonlinear interactions of micro and semi-micro fluctuations

3.2.1 Set of moment equations

The closed set of equations for the relevant quantities (amplitudes I_1^h and I_1^l , eddy damping rates γ_v^h and γ_v^l , and the inverse of auto-correlation times λ^h and λ^l , for the micro and semi-micro fluctuations, respectively) are obtained:

Extended fluctuation dissipation relations from Eqs.(78) and (83);

$$\Re(\lambda^l) I^l = \frac{C_0^l}{2} \gamma_v^l I^l + \frac{\hat{C}_0^h}{2} \gamma_v^h \left(\frac{k_0^l}{k_0^h} \right)^4 I^h, \quad (\text{semi-micro}) \quad (139)$$

$$\Re(\lambda^h) = \frac{C_0^h}{2} \gamma_v^h, \quad (\text{micro}) \quad (140)$$

the renormalization relation for eddy-damping rate from Eqs.(80), (81);

$$\gamma_v^l (\gamma_v^{l*} + \gamma_{vc}^l) = (k_0^l)^4 I^l + (k_0^l)^2 (k_0^h)^2 \frac{\gamma_v^{l*} + \gamma_{vc}^l}{\gamma_v^{h*} + \gamma_{vc}^h} I^h, \quad (\text{semi-micro}) \quad (141)$$

$$\gamma_v^h (\gamma_v^{h*} + \gamma_{vc}^h) = (k_0^h)^4 I^h, \quad (\text{micro}) \quad (142)$$

and the eigenvalues for renormalized operator from Eqs.(110) and (138);

$$\Re \lambda^l = - \frac{\gamma_0^l}{1 + (\omega_{E1}/\omega_{Ec}^l)^2} + \gamma_v^l, \quad (\text{semi-micro}) \quad (143)$$

$$\Re \lambda^h = - \frac{\gamma_0^h \sqrt{1 + |k_0^{l*2}/2\gamma_v^l|} \sqrt{I^l}}{1 + (\omega_{E1}/\omega_{Ec}^h)^2 + (k^l)^4 (\omega_{Ec}^h)^{-2} I^l} + \gamma_v^h. \quad (\text{micro}) \quad (144)$$

Here, the fluctuation amplitude is represented for the electrostatic potential and we write

$$I^{l,h} = I_1^{l,h}. \quad (145)$$

The term γ_v is the characteristic eddy-damping rate of the perpendicular ion motion, and k_0^l and k_0^h are the characteristic wave numbers of the semi-micro and micro modes, respectively. Figure 3 summarizes the nonlinear interactions in turbulent fluctuation which is composed of the semi-micro mode and micro mode.

3.2.2 Strong turbulence limit

Self-consistent solution for the nonlinearly interacting multiple-scale fluctuations is studied in the strong turbulence limit

$$\gamma_v^{h,l} \gg \gamma_{vc}^{h,l} \quad (146)$$

and

$$I^{h,l} \gg \text{thermal fluctuations} \quad (147)$$

We consider the case where the ordering

$$(k_0^l)^2 \ll (k_0^h)^2 \quad (148)$$

holds.

In the limiting case of Eqs.(146) and (147), the renormalization relation Eq.(142) is rewritten as

$$\frac{\gamma_v^h}{k_0^{h2}} \approx \sqrt{I^h} \quad (\text{micro mode}) \quad (149)$$

Substituting of Eq.(149) into Eq.(141) with relation Eq.(146), one has the renormalization relation for the semi-micro mode as

$$\frac{\gamma_v^l}{k_0^{l4}} \approx I^l + \frac{\gamma_v^l}{k_0^{l2}} \sqrt{I^h} \quad (\text{semi-micro mode}) \quad (150)$$

From Eq.(150), the eddy-damping rate of the semi-micro mode is explicitly given by fluctuation amplitudes of semi-micro and micro modes as

$$\frac{\gamma_v^l}{k_0^{l2}} \approx \frac{\sqrt{I^h} + \sqrt{I^h + 4I^l}}{2} \quad (\text{semi-micro mode}) \quad (151)$$

Equations (149) and (151) represent the relations between the eddy damping rates and fluctuation amplitudes.

3.2.3 Extended fluctuation dissipation theorem for semi-micro mode

Extended fluctuation-dissipation relation is solved for the semi-micro mode. Substituting the eddy-damping rate of micro mode (149) and the nonlinear eigenvalue relation Eq.(143) into Eq.(139), the extended FDT is rewritten as

$$\left(-\frac{1}{k_0^{l2}} \frac{\gamma_0^l}{1 + (\omega_{E1}/\omega_{Ec}^l)^2} + \frac{\gamma_v^l}{k_0^{l2}} \right) I^l = \frac{C_0^l}{2} \frac{\gamma_v^l}{k_0^{l2}} I^l + \frac{\hat{C}_0^h}{2} \left(\frac{k_0^l}{k_0^h} \right)^2 (I^h)^{3/2} \quad (152)$$

One obtains from Eq.(152) the equation which the fluctuation level must satisfy as

$$\frac{\gamma_v^l}{k_0^{l2}} I^l = D^l I^l + \varepsilon (I^h)^{3/2} \quad (153)$$

where

$$D^l = \frac{2}{2 - C_0^l} \frac{1}{k_0^{l^2}} \frac{\gamma_0^l}{1 + (\omega_{E1}/\omega_{Ec}^l)^2} . \quad (154)$$

In this expression, D^l denotes the magnitude of the driving power by the global inhomogeneity, and is the characteristic value of the diffusivity by the semi-micro mode. This form of D^l includes the enhancement by the self-nonlinear noise [8]. (Notice that the characteristic scale length $(k_0^l)^{-1}$ is determined by the nonlinear theory Eq.(49).) In the absence of the mutual nonlinear interactions with micro mode fluctuations, $I^h \rightarrow 0$, in Eqs.(151) and (153), one has

$$I^l = (D^l)^2 . \quad (155)$$

The smallness parameter

$$\varepsilon = \frac{\hat{C}_0^h}{2 - C_0^l} \left(\frac{k_0^l}{k_0^h} \right)^2 . \quad (156)$$

represents the coupling coefficient for the drive of the semi-micro mode by the nonlinear noise of micro mode.

Substituting the expression of γ_v^l of Eq.(151) into Eq.(153), one obtains

$$\left(\frac{\sqrt{I^h} + \sqrt{I^h + 4I^l}}{2} - D^l \right) I^l = \varepsilon (I^h)^{3/2} . \quad (157)$$

This equation shows the relation between the fluctuation level I^l and that of the micro mode I^h , the driving parameter D^l and the coupling parameter ε . Example of the fluctuation level I^l as a function of I^h is illustrated in Fig.4(a) for fixed parameter ε , where quantities are normalized to D^l . If the level of micro mode is small,

$$I^h < D^{l^2} , \quad (158)$$

I^l takes a finite value of the order D^l , and is a decreasing function of I^h . For a fixed value of I^h , the semi-micro mode amplitude increases together with D^l , i.e., the mode is excited by the (linear and/or nonlinear) semi-micro instabilities. In contrast, if the level of micro mode is high,

$$I^h > D^{l2} \quad (159)$$

the semi-micro mode is quenched and the amplitude is of the order of ϵ . In this parameter regime, the level I^l is an increasing function of I^h , which is shown in Fig. 4(b). That is, the semi-micro mode is excited only through the noise excitation by the micro-mode.

Two limiting analytic forms of I^l , as a function of I^h , are derived. Equation (157) shows that the left hand side is $O(\epsilon)$. This means that either $\left(\sqrt{I^h}/2 + \sqrt{I^h + 4I^l}/2 - D^l \right)$ or I^l goes to zero in the limit of $\epsilon \rightarrow 0$. If the amplitude of semi-micro mode is not small

$$I^l \gg \epsilon I^h, \quad (160)$$

the first term in the left hand side of Eq.(157) is $O(\epsilon)$, i.e.,

$$\frac{\sqrt{I^h} + \sqrt{I^h + 4I^l}}{2} = D^l + O(\epsilon) \quad (161)$$

One has a relation for the fluctuation level

$$I^l = D^{l2} - D^l \sqrt{I^h} + O(\epsilon). \quad (162)$$

This relation represents the regime of Eq.(158) in Fig.4(a), where I^l is a decreasing function of I^h . In this case, the eddy damping rate and the decorrelation rate (the inverse of the autocorrelation time) of the semi-micro mode are given as

$$\gamma_v' = D^l k_0^{l2} + O(\epsilon), \quad (163)$$

and

$$\Re \lambda^l = \frac{C_0^l}{2} D^l k_0^{l2} + O(\epsilon). \quad (164)$$

Even though the level is influenced by the micro mode amplitude I^h , the decorrelation rate is mainly controlled by the driving parameter of the semi-micro mode. In other limit, where I^l is small,

$$I^l/I^h \sim O(\epsilon), \quad (165)$$

the term $\left(\sqrt{I^h}/2 + \sqrt{I^h + 4I^l}/2 - D^l\right)$ in Eq.(157) is approximated as $\left(\sqrt{I^h} - D^l\right)$, and Eq.(157) provides the relation which is valid in the range $\sqrt{I^h} > D^l$ as

$$I^l = \epsilon \left(\frac{\sqrt{I^h}}{\sqrt{I^h} - D^l} \right) I^h \sim \epsilon I^h. \quad (166)$$

In this case, the eddy damping rate and decorrelation rate are given as

$$\gamma_v^l = \sqrt{I^h} k_0^{l^2} + O(\epsilon) \quad (167)$$

and

$$\Re \lambda^l = \frac{C_0^l}{2} \sqrt{I^h} k_0^{l^2} + O(\epsilon). \quad (168)$$

Equations (166), (167) and (168) show that not only the fluctuation level I^l but also the eddy damping rate and decorrelation rate are governed by the level of micro mode I^h .

The decorrelation rate $\Re \lambda^l$ is greater than $D^l k_0^{l^2}$.

3.2.4 Extended fluctuation dissipation theorem for micro mode

Extended fluctuation-dissipation theorem for the micro mode Eq.(140) with the nonlinear eigenvalue equation Eq.(144) and the renormalization relation Eq.(149) provide the fluctuation level,

$$I^h \simeq \gamma_v^{h^2} k_0^{h-4} = \left(\frac{\gamma_0^h}{k_0^{h^2}} \frac{2}{2 - C_0^h} \frac{\sqrt{1 + |k_0^{l^2}/2\gamma_v^l| \sqrt{I^l}}}{1 + (\omega_{E1}/\omega_{Ec}^h)^2 + (k^l)^4 (\omega_{Ec}^h)^{-2} I^l} \right)^2, \quad (169)$$

the eddy-damping rate

$$\gamma_v^h = \frac{2}{2 - C_0^h} \frac{\sqrt{1 + |k_0^{l^2}/2\gamma_v^l| \sqrt{I^l}}}{1 + (\omega_{E1}/\omega_{Ec}^h)^2 + (k^l)^4 (\omega_{Ec}^h)^{-2} I^l} \gamma_0^h, \quad (170)$$

and the decorrelation rate (the inverse of the autocorrelation time)

$$\Re \lambda^h = \frac{C_0^h}{2} \gamma_v^h = \frac{C_0^h}{2 - C_0^h} \frac{\sqrt{1 + |k_0^l|^2/2\gamma_v^l} \sqrt{I^l}}{1 + (\omega_{E1}/\omega_{Ec}^h)^2 + (k^l)^4 (\omega_{Ec}^h)^{-2} I^l} \gamma_0^h \quad (171)$$

as functions of the magnitude of the semi-micro mode turbulence I^l and the global driving parameters. In a normalized representation, Eq.(169) is rewritten as

$$I^h = (D^h)^2 \frac{1 + |k_0^l|^2/2\gamma_v^l} {(1 + I_{eff}^{-1} I^l)^2} \sqrt{I^l} \quad (172)$$

where

$$D^h = \frac{2}{2 - C_0^h} \frac{1}{1 + (\omega_{E1}/\omega_{Ec}^h)^2} \frac{\gamma_0^h}{k_0^{h2}}, \quad (173)$$

and

$$I_{eff} \equiv \left(1 + (\omega_{E1}/\omega_{Ec}^h)^2\right) (\omega_{Ec}^h)^2 (k^l)^{-4}. \quad (174)$$

D^h is the characteristic diffusion rate, being represented by the magnitude of the drive for the micro mode. The parameter I_{eff} denotes the level of turbulence of the semi-micro mode, at which the suppression of micro mode is effectively induced. In the absence of the coupling between the semi-micro mode, one has the amplitude for micro mode,

$$I^h = (D^h)^2. \quad (175)$$

In the presence of the coupling, eliminating γ_v^l from Eq.(172) by use of Eq.(151), one has

$$I^h = (D^h)^2 \frac{1}{(1 + I_{eff}^{-1} I^l)^2} \left(1 + \frac{\sqrt{I^l}}{\sqrt{I^h} + \sqrt{I^h + 4I^l}}\right) \quad (176)$$

showing the influence of the semi-micro mode level I^l on the micro mode fluctuations I^h . This equation includes the driving parameter for the micro mode D^h and the parameter I_{eff} .

Figure 5 illustrates the level I^h as a function of the level I^l for given global parameters. The quantities are normalized to D^h (in Fig.5). In the limit of small amplitude of the semi-micro mode, the fluctuation level I^h increases as I^l increases. This is due to the local steepening of the pressure gradient by the semi-micro mode. In the limit $I^l \ll (D^h)^2$, Eq. (176) gives an approximate relation

$$I^h = (D^h)^2 \left(1 + \frac{\sqrt{I^l}}{2D^h} \right) \quad (177)$$

However, if the fluctuation level of semi-micro mode becomes higher, the suppression by the flow shear dominates. Then the level I^h starts to decrease for increasing I^l . In the limit of $I^l \gg I^h$, (i.e., $I^l \left(1 + I_{eff}^{-1} I^l \right)^2 \gg (D^h)^2$) the last term in the right hand side of Eq.(176) converges to $3/2$, and Eq.(176) is approximated as

$$I^h = (D^h)^2 \frac{3}{2 \left(1 + I_{eff}^{-1} I^l \right)^2} \quad (178)$$

The level of micro mode I^h decreases as I^l increases.

3.3 Self-consistent solution, bifurcation and phase diagram

The relation of the semi-micro mode, Eq.(157) and the one for the micro mode Eq.(176) must be simultaneously satisfied. Combining these equations, the self-consistent solution is obtained. This system is characterized by parameters D^l , D^h , I_{eff} and ϵ . The parameters D^l and D^h represent the magnitude of the drive by global inhomogeneity, and are the turbulence transport coefficients without the mutual interactions. The parameter I_{eff} stands for the critical strength of the nonlinear interactions between semi-micro fluctuations and micro fluctuations. The parameter ϵ represents the magnitude of the noise pumping for the semi-micro mode by micro mode noise.

3.3.1 Self-consistent solution

Self-consistent solutions for Eqs.(157) and (176) are investigated, and the dependence on the coupling parameters I_{eff} and ϵ is studied.

We first study the case where the threshold for the suppression of micro mode I_{eff} is high, $I_{eff} \gg D^{h,l}$. In this case, Eq.(176) shows that the level of micro mode I^h is weakly dependent on the level of semi-micro mode I^l . Figure 6 shows the relations between the levels of semi-micro mode and micro mode, Eqs.(157) and (176), on the

(I^l, I^h) plane. The extended FDT of the micro mode Eq.(176) is denoted by the solid line, and that of the semi-micro mode Eq.(157) is shown by dotted and broken lines. In this graph, the axis is normalized by the unperturbed level $(D^h)^2$. The drive for the micro mode is fixed, and that for semi-micro mode D^l is varied, and the relation Eq.(157) is plotted for various values of D^l . The cross point represents the self-consistent solution. As is shown in Fig.4, the relation Eq.(157) has two limiting forms, and the curve of Eq.(157) changes the characteristic feature near the condition $I^h \approx \sqrt{D^l}$. Depending on the ratio of D^l/D^h , the nature of the solution changes.

Let us examine two cases of $D^l > D^h$ and $D^l < D^h$. If the drive of semi-micro mode D^l is large enough to exceed the threshold,

$$D^l > D^h, \quad (179)$$

the solution for which semi-micro mode is strongly excited appears. The cross point in Fig.6 exists in the region where I^l has large value. The solution in the branch of Eq.(162) is realized. In the large D^l limit, $D^l \gg D^h$, one has

$$I^l \approx D^{l2} \quad (180)$$

and

$$I^h \approx D^{h2} I_{eff}^2 I^{l-2} \approx D^{h2} I_{eff}^2 D^{l-4}. \quad (181)$$

As D^l increases, the level of I^l increases; however, I^h starts to decrease.

When the drive for the semi-micro mode is weak,

$$D^l < D^h, \quad (182)$$

the self-consistent solution is realized in the limit of Eq.(166). We have

$$I^h \approx (D^h)^2, \quad (183)$$

and

$$I^l \approx \epsilon I^h. \quad (184)$$

The micro mode turbulence is excited. Although the drive D^l is finite, semi-micro mode instabilities do not grow and is quenched, being only excited through the noise pumping by the micro mode. The eddy damping due to the micro mode is large.

The level of self-consistent solution is given in Fig.7 as a function D^l . The threshold for the excitation of the semi-micro mode is observed. In the case of Fig.7, where $I_{eff} \gg D^{h,l}$ holds and the $E \times B$ shearing effect is weak, the transition of the dominant solution turns out to be a soft transition.

3.3.2 Bifurcation

Self-consistent solutions for Eqs.(157) and (176) can be multiple and show the hard bifurcation.

Figure 8 shows that the multiple solutions exist. If the drive for the semi-micro mode D^l is strong, (e.g., the dotted-dashed line), the solution exists in the limit of Eq.(162) as is denoted by 'S'. ('S' stands for 'semi-micro' mode.) When the drive D^l becomes weaker, the solution 'S' disappears, and the solution is realized by the limit of Eq.(166), i. e., the solution 'M' appears. ('M' stands for 'micro' mode.) In the solution 'S', the semi-micro mode is strongly excited and the micro mode is suppressed. In the solution 'M', the micro mode is excited, but the semi-micro mode is quenched. For the intermediate values of the drive D^l , the multiple solutions of 'S' and 'M' exist simultaneously.

Figure 9 illustrates the fluctuation amplitudes as a function of the driving ratio D^l/D^h . When $D^l/D^h < 1$, only the solution 'M', Eqs.(183) and (184), is given. The micro mode is excited, but the semi-micro mode is quenched, and the amplitude I^l is little influenced by the drive of the semi-micro mode D^l . When the drive D^l exceeds the critical value, the solution 'S' (given by Eqs.(180) and (181)) also appears. As the drive D^l increases, I^l increases but I^h is more strongly suppressed. Owing to the coexistence of two solutions, a hysteresis appears in the relation between the gradient and fluctuation level. At the critical point, the transition from solution 'S' to 'M' (or 'M' to 'S') takes place.

3.3.3 Phase diagram

The presence of hard bifurcation in the fluctuation level forms a cusp type catastrophe in the phase diagram represented by the two parameters D^l and D^h .

The threshold condition for the solution 'M' to exist is given as

$$D^l < D^h. \quad (185)$$

The threshold condition for the solution 'S' is also estimated. Neglecting a weak dependence on I^l in the last term in the right hand side of Eq.(176), Eq.(176) is approximately given as

$$\sqrt{I^h} \approx \frac{D^h}{1 + I_{eff}^{-1} I^l} . \quad (186)$$

Combining Eqs.(162) and (186), the condition for 'S' to exist is obtained as,

$$D^h < \frac{1}{4 D^l I_{eff}} \left(D^{l2} + I_{eff} \right)^2 . \quad (187)$$

From Eqs.(185) and (187), one sees that the two solutions 'S' and 'M' can appear simultaneously in the cusp region

$$D^l < D^h < \frac{1}{4 D^l I_{eff}} \left(D^{l2} + I_{eff} \right)^2 . \quad (188)$$

The critical point of the cusp is given as

$$D^l = D^h = \sqrt{I_{eff}} . \quad (189)$$

In the limit of strong drive,

$$D^l \gg \sqrt{I_{eff}} , \quad (190)$$

the cusp region Eq.(188) takes an asymptotic form as

$$\left(4 I_{eff} D^h \right)^{1/3} < D^l < D^h . \quad (191)$$

Figure 10 illustrates the phase diagram for the turbulence which is composed of the semi-micro mode and micro mode.

As is discussed in literature, amplitude $\sqrt{I^h}$ or $\sqrt{I^l}$ is the turbulent transport coefficient. Therefore Fig. 10 also represents the cusp type catastrophe of the turbulent transport.

3.3.4 Test particle diffusion

Equation (88) gives an estimate of the test particle diffusion. The test particle diffusion coefficient associated with the solutions 'S' and 'M' can be calculated.

On the branch 'S', in which the semi-micro mode is strongly excited, the decorrelation rate for the semi-micro mode is given by Eq.(164), i.e.,

$$\Re \lambda^l \simeq \frac{C_0^l}{2} D^l k_0^{l^2}. \quad (192)$$

The fluctuation level of the semi-micro mode is given as Eq.(180), $I^l \simeq D^{l^2}$. By using Eqs.(180) and (192), the contribution from the semi-micro mode to the test particle diffusion coefficient is given as

$$\frac{(k_0^l)^2}{\Re \lambda^l} I^l = \frac{2}{C_0^l} \frac{I^l}{D^l} \simeq \frac{2}{C_0^l} D^l. \quad (193)$$

As for the micro mode, Eqs.(140) and (149) give the estimate

$$\Re \lambda^h = \frac{C_0^h}{2} \sqrt{I^h} (k_0^h)^2, \quad (194)$$

i.e.,

$$\frac{(k_0^h)^2}{\Re \lambda^h} I^h \simeq \frac{2}{C_0^h} \sqrt{I^h}. \quad (195)$$

The contribution from the micro mode to the test particle diffusivity is given, by substituting the fluctuation level Eq.(181) into Eq.(195), as

$$\frac{(k_0^h)^2}{\Re \lambda^h} I^h \simeq \frac{2}{C_0^h} D^h I_{eff} (D^l)^{-2}, \quad (196)$$

in the limit of $D^l \gg D^h$. Summing up Eqs.(193) and (196), one has the test particle diffusivity for the solution 'S' as

$$D_{test} \simeq \frac{2}{C_0^l} D^l + \frac{2}{C_0^h} D^h I_{eff} D^{l-2}. \quad (D^l \gg D^h) \quad (197)$$

The micro mode level is suppressed by the semi-micro mode activity. The coefficient D_{test} increases as the drive for the semi-micro mode D^l increases.

On the branch 'M', the turbulent transport is mainly driven by the micro mode. The level and the decorrelation rate of the micro mode are given by Eqs.(183) and (194), respectively. Substituting Eq.(183) into Eq.(195), the contribution of the micro-mode to the test particle diffusion is estimated as

$$\frac{(k_0^h)^2}{\Re \lambda^h} I^h \simeq \frac{2}{C_0^h} D^h. \quad (198)$$

The decorrelation rate and amplitude of the semi-micro mode is given by Eqs.(166) and (168), respectively. The contribution of the semi-micro mode is given as

$$\frac{(k_0^l)^2}{\Re \lambda^l} I^l \simeq \frac{2}{C_0^l} \varepsilon \sqrt{I^h} \simeq \frac{2}{C_0^l} \varepsilon D^h. \quad (199)$$

The semi-micro mode influences on the test particle diffusion at the order of smallness parameter $\varepsilon \simeq O\left((k_0^l/k_0^h)^2\right)$. It is also noted that the magnitude is controlled by the parameter D^h . Combining Eqs.(198) and (199), the test particle diffusion coefficient is given as

$$D_{test} \simeq \frac{2}{C_0^h} D^h + O(\varepsilon). \quad (200)$$

The diffusion coefficient is determined by the drive of the micro mode D^h , and is independent of the drive for the semi-micro mode D^l .

Figure 11 illustrates an example for the test particle diffusion coefficient as a function of the drive of the semi-micro mode. In Fig.11(a), i.e., the case of hard transition, the solid line is for the branch 'S' and the dashed line is for the branch 'M'. The case of soft transition is illustrated in Fig.11(b). In the case of the weak drive of the semi-micro mode, the diffusion coefficient is given as Eq.(200). In the large drive limit, it increases in proportion to D^l .

3.4 Impact of global electric field shear

The global radial electric field introduces new dynamical transitions in the presence of nonlinear interactions between fluctuations of different scale length.

When the nonlinear interactions between different fluctuations are neglected, the inhomogeneous radial electric field suppresses the fluctuations as

$$D^l \propto \frac{1}{1 + (\omega_{E1}/\omega_{Ec}^l)^2} \quad (201a)$$

$$D^h \propto \frac{1}{1 + (\omega_{E1}/\omega_{Ec}^h)^2} . \quad (201b)$$

The fluctuation levels decrease as the radial electric field shear, denoted by ω_{E1} , increases.

In the presence of nonlinear interactions, depending on the ratio $\omega_{Ec}^l/\omega_{Ec}^h$, different types of bifurcation appear.

Under many circumstances, the suppression of turbulence by flow shear is easier for the semi-micro mode,

$$\omega_{Ec}^l \leq \omega_{Ec}^h . \quad (202)$$

For the examples in this article, Eqs (107) and (108) provide

$$\omega_{Ec}^l \sim sv_{th}^l/qR \quad \text{and} \quad \omega_{Ec}^h \sim sv_{th}^h/\sqrt{a}R , \quad (203)$$

satisfying Eq.(202). If Eq.(202) holds and other parameters are fixed, the driving parameter for the semi-micro mode $D^l(\omega_{E1})$ decreases faster than that of micro mode $D^h(\omega_{E1})$ as the shear of global radial electric field increases. The trajectories on the phase diagram $(D^l(\omega_{E1}), D^h(\omega_{E1}))$ are given by the solid lines (A-A', or B-B') in Fig.12. Points A and B denote the states in the absence of the electric field shear, $\omega_{E1} = 0$, and $D^l(\omega_{E1})$ and $D^h(\omega_{E1})$ are reduced as ω_{E1} increases from $\omega_{E1}/\omega_{Ec}^l = 0$ to $\omega_{E1}/\omega_{Ec}^l = 2$. Other global parameters are fixed along the trajectory.

In the case of A-A', the initial state (A) is taken in the domain where the semi-micro mode is strongly excited, while the micro mode is suppressed. When the electric field shear ω_{E1} is increased, the semi-micro mode starts to be suppressed by the electric field shear. The micro mode, however, starts to be enhanced, because the suppression by the semi-micro mode is reduced. The reduction of suppression by semi-micro mode is stronger than the reduction of the drive by the global electric field shear. When the trajectory crosses the phase boundary (point C in Fig.12),

$$D^h = \frac{1}{4 D^l I_{eff}} (D^{l2} + I_{eff})^2 , \quad (204)$$

the phase transition of turbulence takes place. The semi-micro mode is quenched by the dissipation of the micro mode, and the level of micro fluctuations jumps up. In the domain of micro mode, the level of micro fluctuations starts to decrease. Figure 13(a) illustrates the fluctuation amplitudes $\sqrt{I^l}$ and $\sqrt{I^h}$ as a function of ω_{E1} , when it is increased. A hard type bifurcation is observed.

Owing to the nature of hard transition with hysteresis, the back transition takes place not at point C but at C', when the global electric field shear reduces from $\omega_{E1}/\omega_{Ec}^l = 2$ to $\omega_{E1}/\omega_{Ec}^l = 0$ (from A' to A in Fig.12). At the point C', the condition

$$D^l(\omega_{E1}) = D^h(\omega_{E1}) \quad (205)$$

holds. Figure 13(b) shows the level of micro and semi-micro fluctuations as a function of ω_{E1} in the case of decreasing ω_{E1} . Figure 13(c) demonstrates the hysteresis of the fluctuation level.

In the case of weak drive (B-B' in Fig.12), the change is much smoother. Across the phase boundary Eq.(205), the semi-micro mode is either excited or quenched, and the change of the micro fluctuation is smooth. The bifurcation is soft. Figure 14 is one example for the case of increasing ω_{E1} , showing the soft transition.

3.5 Multiple classes of fluctuations

The closed set of equations for the case where turbulence is composed of two classes of fluctuation modes is obtained as Eqs.(139)-(144). The result can be extended to more general cases. Let us consider the case where the turbulence is composed of N classes of fluctuation modes. We assume that the scale length separation and time scale separation hold among them, i.e.,

$$k_0^{(1)2} \ll k_0^{(2)2} \ll \dots \ll k_0^{(n)2} \ll \dots \ll k_0^{(N)2} \quad (206a)$$

$$(n = 1, \dots, N)$$

$$\gamma_b^{(1)} \ll \gamma_b^{(2)} \ll \dots \ll \gamma_b^{(n)} \ll \dots \ll \gamma_b^{(N)} \quad (206b)$$

where the superscript (n) indicates the n -th mode composing the turbulence and $k_0^{(n)}$ is the characteristic wave number of the n -th mode. Analyses in §2 and §3 are developed for the case of $N = 2$ and symbols $(1) = l$ and $(2) = h$ are used. As is the case of $N = 2$, the statistical independence among different class of modes is assumed, based upon the scale separations.

As is the case of §3, nonlinear influences on the n -th mode from the other n' -th modes are decomposed as the eddy damping and noise excitation by the smaller scale (higher mode numbers) fluctuations $n' > n$, and as the suppression through shearing and

drive through the local pressure steepening by the larger scale (lower mode numbers) fluctuations, $n' < n$. Figure 15 illustrates these nonlinear interactions from different modes. On the basis of the assumption of statistical independence, influences are given as a sum of effects of the other modes. Self-nonlinear effect is unchanged. The equations for relevant quantities (amplitudes $I^{(n)}$, eddy damping rate $\gamma_b^{(n)}$, and decorrelation rate $\Re \lambda^{(n)}$) are obtained:

Extended fluctuation dissipation theorem;

$$\Re(\lambda^{(n)}) I^{(n)} = \frac{C_0^{(n)}}{2} \gamma_b^{(n)} I^{(n)} + \sum_{n'=n+1}^N \frac{\hat{C}_0^{(n')}}{2} \gamma_b^{(n')} \left(\frac{k_b^{(n)}}{k_b^{(n')}} \right)^4 I^{(n')}, \quad (n = 1, \dots, N-1) \quad (207)$$

$$\Re(\lambda^{(N)}) = \frac{C_0^{(N)}}{2} \gamma_b^{(N)}, \quad (208)$$

the renormalization relation for eddy-damping rate in the strong turbulence limit;

$$\gamma_b^{(n)2} = (k_b^{(n)})^4 I^{(n)} + (k_b^{(n)})^2 \sum_{n'=n+1}^N (k_b^{(n')})^2 \frac{\gamma_b^{(n)}}{\gamma_b^{(n')}} I^{(n')}, \quad (n = 1, \dots, N-1) \quad (209)$$

$$\gamma_b^{(N)2} = (k_b^{(N)})^4 I^{(N)}, \quad (210)$$

and the eigenvalues for renormalized operator;

$$\Re \lambda^{(1)} = - \frac{\gamma_b^{(1)}}{1 + (\omega_{E1}/\omega_{Ec}^{(1)})^2} + \gamma_b^{(1)}, \quad (211)$$

$$\Re \lambda^{(n)} = - \frac{\gamma_b^{(n)} \sqrt{1 + \sqrt{\sum_{n'=1}^{n-1} \left| k_b^{(n')2}/2\gamma_b^{(n')} \right|^2 I^{(n')}}}}{1 + (\omega_{E1}/\omega_{Ec}^{(n)})^2 + (\omega_{Ec}^{(n)})^{-2} \sum_{n'=1}^{n-1} (k_b^{(n')})^4 I^{(n')}} + \gamma_b^{(n)}, \quad (n = 2, \dots, N) \quad (212)$$

where $\gamma_b^{(n)}$ is the eigenvalue in the absence of the sheared $E \times B$ flow and mutual interactions between different modes.

4. Application to Transient Transport Problems

The statistical theory of the multiple-scale fluctuations is applied to the transient transport problems in toroidal plasmas.

4.1 Transient transport problem

It has been well known in experiments that the estimate of thermal diffusivity based on the stationary energy balance, χ_{pb} , and the one based on the transient response like heat pulse propagation, χ_{Hp} , have shown unambiguous discrepancy [25]. The latter is usually larger than the former. This discrepancy is partly understood by noting the explicit dependence of χ_{pb} on the temperature gradient. If it has a dependence like

$$\chi \propto |\nabla T|^\alpha, \quad (213)$$

the effective thermal diffusivity measured by heat pulse propagation satisfies

$$\chi_{Hp} \approx (1 + \alpha) \chi_{pb}. \quad (214)$$

However, this does not suffice. For instance, the change of thermal diffusivity in the core plasma after the onset of L/H transition at edge requires $\alpha \sim 50$ in order to explain the observation on JET [44]. The value $\alpha \sim 50$ contradicts to the transport property in stationary state, which requires $\alpha = 1 \sim 3/2$. In addition, a hysteresis relation in the local gradient and local heat flux has been reported from W7-AS experiments. In order to understand these transient transport problems, a non-local model of heat flux has been proposed [45]. This model assumes the existence of the fluctuations with long radial correlation length of the order of the minor radius. Therefore, the heat flux at some location is a sum of the local heat flux and an integral over the range of long correlation length. This model has successfully explained several features of the transient transport problems [45, 46]. However, the physics basis for the fluctuations with long correlation length has not been given. The mode with long radial correlation length corresponds to low poloidal mode numbers, and such mode is usually stable. The statistical theory in the turbulent plasmas allows to calculate the level of long-wave-length fluctuations which are excited by the random noise of micro turbulence.

4.2 Long-wave-length fluctuations

4.2.1 Noise-induced fluctuations

Fluctuations of the long-wave-length mode of the order of minor radius in background micro fluctuations are considered. Schematic drawing is given in Fig.16. The semi-micro mode and micro mode, which are driven by global inhomogeneities and

induce turbulent transport, are categorized as microscopic modes in this section. Long-wave-length modes and microscopic modes are considered to coexist in the plasma. We investigate here the case where the long-wave-length mode is stable, and such fluctuations are excited by the nonlinear noise from microscopic fluctuations.

According to the extended Fluctuation Dissipation Theorem, its fluctuation level and associated thermal flux have been given as

$$\langle \tilde{\Phi}_\ell^* \tilde{\Phi}_\ell \rangle = \frac{1}{2\lambda_\ell} |A_{\ell, 11}|^2 \langle \tilde{S}^* \tilde{S} \rangle \quad (215)$$

and

$$q_\ell = - \sum_\ell \frac{k_{\ell, y}^2}{\gamma_{\ell, p} - \lambda_\ell} \frac{1}{2\lambda_\ell} |A_{\ell, 11}|^2 \langle \tilde{S}^* \tilde{S} \rangle p'_0 \quad (216)$$

where the suffix ℓ indicates the long-wave-length mode, λ_ℓ is the eigenvalue of the nonlinear decorrelation rate, \mathbf{A}_ℓ is the projection operator, and \tilde{S} is the nonlinear noise for the long-wave-length mode, respectively. The over-bar denotes the integral over the correlation length of the ℓ -mode. This level of Eq.(215) is the statistical average of the amplitude, and radial shape is given by eigenmode in toroidal plasmas.

4.2.2 Estimate of noise source

By use of the estimate of previous sections, Eq.(73), the nonlinear noise which is driven by the background microscopic turbulence is given as

$$\langle S_\ell^* S_\ell \rangle = \hat{C}_0^h \gamma_v^h \frac{p^2}{k^4} |A_{\ell, 11}|^{-2} I^h \quad (217)$$

where p is the wave number of the long-wave-length mode, and k and I^h are the wave number and the level of the potential perturbation, respectively, associated with the background microscopic mode fluctuations. (k_0^h in Eq.(73) is simply written as k .) We assume that the relation

$$|p| \ll |k| \quad (218)$$

holds. The turbulent transport coefficient which is induced by the microscopic mode fluctuations, χ_{turb} , is related with I^h in the strong turbulence limit as

$$I^h \simeq \chi_{turb}^2. \quad (219)$$

By use of this relation Eq.(219), the noise source amplitude in Eq.(217) is estimated as

$$\langle S^* S \rangle \simeq C_0 \gamma_k p^2 k^{-4} \chi_{turb}^2 . \quad (220)$$

It is convenient to rewrite Eq.(220) as

$$\langle S^* S \rangle \simeq \hat{C}_0^h \gamma_v^{h2} p^2 k^{-6} \chi_{turb} , \quad (221)$$

where the estimate

$$\gamma_v^h \simeq \chi_{turb} k^2 \quad (222)$$

is used.

4.2.3 Nonlocal heat flux

Combining the noise source amplitude Eq.(221) with the heat flux formula Eq.(216), one has the heat flux which is induced by the long-wave-length fluctuations as

$$q_\ell \simeq - \sum_\ell \frac{\hat{C}_0^h p_y^2 p^2}{k^6} \left(\frac{\gamma_k^h}{\lambda_\ell} \right)^2 \chi_{turb} p_0' . \quad (223)$$

The decorrelation rate of the long-wave-length mode , λ_ℓ , is obtained by solving the nonlocal nonlinear eigenmode equation in the presence of the background microscopic mode turbulence. An example for the low-poloidal-mode-number modes in helical plasmas has been analyzed in [47]. An analytic form of the decorrelation rate has been discussed, but we here consider the limit where the long-wave-length is stable and the level is low. In the low-amplitude limit, the decorrelation rate is given as [47]

$$\lambda_\ell \simeq \chi_{turb} p^2 . \quad (224)$$

Substitution of Eqs.(222) and (224) into Eq.(223) yields

$$q_\ell \simeq - \sum_\ell \frac{\hat{C}_0^h}{k^2} \chi_{turb} p_0' \sim - p^2 k^{-2} \chi_{turb} p_0' . \quad (225)$$

It is noted that this heat flux is the lower bound of the heat flux which is driven by the long-wave-length fluctuations. This is because, (i) the contribution of the self-nonlinear

noise is neglected and (ii) the decorrelation rate Eq.(224) is evaluated at the most stable limit.

4.3 Impact on transient transport problem

The result Eq.(225) gives an insight into the transient transport problems.

First, this heat flux is small in stationary state in comparison with the local heat flux which is driven by the microscopic turbulence. The latter is given as $-\chi_{turb} p_0'$. The nonlocal heat flux is about $p^2 k^{-2}$ times smaller than that in the stationary state. This result in the stationary state agrees with the analysis in § 3. Comparing Eqs.(198) and (199), one sees that when the longer-scale-length mode is excited through the nonlinear noise of the shorter-scale-length mode, the contribution of the former to the transport is $\varepsilon \simeq O\left((k_0^l/k_0^h)^2\right)$ times smaller than that of the latter.

However, the nonlocal heat flux is influential in the transient response. Equation (225) shows that the heat flux changes over the distance of the correlation length, which is of the order of p^{-1} . When the noise source of the eigenmode of the p -mode suddenly changes at a radius, the change of the global mode amplitude appears. The change of mode amplitude propagates across the plasma radius as a response of an radial eigenmode, and reaches the average in an autocorrelation time λ_ℓ^{-1} after a local change happens. That is, the statistical change of the heat flux of Eq.(225) due to the fluctuating global mode is realized in a time interval of λ_ℓ^{-1} . We see that the long-wave-length mode induces, after a local impulse, a statistical change of heat flux, magnitude of which is $(p/k)^2(-\chi_{turb} p_0')$, at a distance of p^{-1} in a time interval of λ_ℓ^{-1} .

This change of heat flux is not a diffusive process. Nevertheless, if one interprets this change as a diffusion process, then this change of heat flux may be attributed to an effective diffusivity χ_{eff} . When a transient delta-function perturbation $X_0\delta(x)$ is given at $t = 0$, the diffusion process gives the perturbation δX , which has a form

$$\delta X \sim X_0 \frac{1}{\sqrt{\chi_{eff} t}} \exp\left(-\frac{x^2}{\chi_{eff} t}\right). \quad (226)$$

The exponential dependence is dominant, and one has $-\ln(\delta X/X_0) \sim x^2/\chi_{eff} t$. Based on this relation, the observed relative change is interpreted by the effective diffusivity as

$$\chi_{eff} = \frac{(\text{distance})^2}{\text{time interval}} \left| \ln(\text{relative change}) \right|^{-1}. \quad (227)$$

Let us estimate χ_{eff} for the nonlocal heat flux of concern. One has distance $\approx 1/p$, time interval $= \lambda_\ell^{-1}$ and relative change $\approx p^2 k^{-2}$. The effective thermal diffusivity is estimated as

$$\chi_{eff} \approx p^{-2} \lambda_\ell \left| \ln(p/k)^2 \right|^{-1}. \quad (228)$$

Substituting Eq.(224) into Eq.(228), one has an effective diffusivity as

$$\chi_{eff} \approx \left| \ln(p/k)^2 \right|^{-1} \chi_{turb}. \quad (229)$$

This value is modified by the factor $\left| \ln(p/k)^2 \right|^{-1}$ from χ_{turb} . This is much larger than the heat diffusivity in a stationary state, since $\left| \ln(p/k)^2 \right|^{-1} \gg p^2 k^{-2}$ holds.

These analyses show that the contribution of the long-wave-length mode, which is excited by the statistical process of micro-turbulence, has strong influence in the response of energy transport after the transient perturbation. This gives an insight the problem of transient transport phenomena in toroidal plasmas, and provides a basis for the nonlocal models for quantitative analysis of experimental observations.

5. Summary and Discussion

In this article, the statistical theory of strong turbulence in inhomogeneous plasmas is extended to analyzing the state where fluctuations with different scale lengths coexist. The nonlinear interactions between micro-mode and semi-micro mode are taken into account. Their interplay (nonlinear dynamics) determines both the fluctuation levels and the cross field turbulent transport. The global parameters are given and fixed here. Fluctuation of the order of Debye length, λ_D , is considered as a thermal fluctuation, and is assumed to be statistically independent of the modes of our concern. The hierarchical structure is constructed for the semi-micro mode, micro mode and thermodynamical fluctuations. A transition in turbulence is found and a phase diagram is drawn with cusp type catastrophe. Generalization for the case where turbulence is composed of N-classes of modes is also developed. The excitation of stable long-wave-length modes by the nonlinear noise of microscopic mode fluctuations (including both micro and semi-micro modes) is investigated. The nonlocal energy flux associated with this process is analyzed.

Nonlinear self-interactions in one class of fluctuation are divided into the coherent drag and the self-noise as has been done in previous analyses I-V. The micro-turbulence of smaller size affects the semi-micro one through the renormalized drag and the nonlinear

noise excitation. The effect of semi-micro turbulence is included in the dynamical equation of the micro-mode as a kind of a driving force or damping force. A set of equations of the fluctuation level and decorrelation rate for the micro and semi-micro fluctuations was obtained. A self-consistent solution for turbulent state was obtained. It is found that there are several states of fluctuations: in one state, the micro mode is excited and the semi-micro mode is quenched; in the other state, the semi-micro mode is excited, and the micro mode is suppressed. A new turbulence transition was obtained, being associated with a hard bifurcation. A phase diagram was obtained. The result clearly shows that the nonlinear interplay is essential in the dynamics of the strong turbulence in inhomogeneous plasmas.

The induced transition of the semi-micro fluctuations sheds a light on the internal transport barrier (ITB) formation. It is widely conjectured that the steep gradient of global radial electric field plays a role in the reduction of the anomalous thermal conductivity. One of the key problems in the ITB formation is the imbalance between the formation of ITB for ion transport and that for electron transport. In many cases, the electron thermal transport remains in the level of L-mode although the thermal barrier for the ion energy is established. The ITB for electron thermal transport can also appear when the ITB for ion energy becomes prominent. This problem has stimulated the studies on the microscopic fluctuations like ETG or CDBM turbulence. The simple addition of the microscopic mode turbulence is not sufficient for the solution of the problem: A reason is as follows. If the semi-micro mode (Like ITG) dominates the anomalous transport in the L-mode as is often discussed, then the dominant electron transport is governed by it. The anomalous ion conductivity and electron conductivity are given as the same order ones. Even though the micro mode presides, the suppression of the dominant semi-micro mode should influence strongly the electron thermal transport as well.

This problem could be solved by considering the transition of the semi-micro and micro turbulence due to their nonlinear interactions. The semi-micro mode induces the ion and electron thermal conductivity (χ_i^l and χ_e^l , respectively) of similar values. It is possible that the turbulence thermal conductivity by the micro mode appears dominantly for electrons, χ_e^h . (E.g., the case of CDBM [38]. So is the case of ETG mode.) As is shown in Fig.13, the suppression of the semi-micro mode could enhance the micro mode. At the transition, the semi-micro mode is almost completely quenched, but the micro mode can jump up to a large amplitude. In the behaviour of the ion thermal conductivity, the transition occurs at a critical value of the gradient of the global $E \times B$ velocity. Above this threshold value, the semi-micro mode is quenched and the ion thermal conductivity decreases strongly. The micro mode fluctuation is enhanced, so that the total electron thermal transport does not decrease much.

The formulation in this article is easily extended to various cases. One application is the analysis of the nonlocal transport problem in §4, which has been analyzed in conjunction with the transient response problems. The contribution of the long-wave-length mode, which is excited by the statistical noise process of micro-turbulence, is obtained. It is shown that small but finite heat flux due to the long-wave-length modes has strong influence in the response of energy transport after the transient perturbation. This gives an insight into the problem of transient transport phenomena in toroidal plasmas, and provides a basis for the nonlocal transport models for quantitative analysis of experimental observations. The problem of the discrepancy between the stationary transport coefficient and that deduced from the transient response is also a common problem for the turbulence in which the Kubo number [48], \mathcal{K} , is much smaller than unity. In strong turbulence of plasma, the condition $\mathcal{K} \approx 1$ usually holds [1]. However, if fluctuations with multiple scale lengths coexist, it is not always the case. When the condition $\mathcal{K} \ll 1$ holds, the correlation length of the perturbed electric field (in Eulerian view) is much longer than the autocorrelation length of plasma motion (in Lagrangian view). In such cases, the transient response could be different from those expected from a simple diffusive model. A detailed analysis will be reported in a forthcoming article.

Acknowledgements

Authors wish to acknowledge Prof. A. Yoshizawa, Prof. R. Balescu, Prof. A. Fukuyama and Dr. M. Yagi for elucidating comments and useful discussions. A part of this work is initiated during the authors' stay at Max-Planck-Institut für Plasmaphysik (IPP), which is supported by the Research-Award Programme of Alexander von Humboldt-Stiftung (AvH). Authors wish to thank the hospitality of Prof. F. Wagner, IPP and AvH. This work is partly supported by the Grant-in-Aid for Scientific Research of Ministry of Education, Culture, Sports Science, and Technology Japan, by the collaboration programme of National Institute for Fusion Science and by the collaboration programme of the Research Institute for Applied Mechanics of Kyushu University.

Appendix A: Five Field Model

The reduced set of equations for the variables of $\{\phi, A_{\parallel}, V_{\parallel}, n, p_i\}$ has been derived [27]. Based on the model in the literature [27] a simplified model is employed. The incompressible limit is chosen for ions and the iso-thermal limit is used for electrons

$$\frac{d}{dt} p_i = 0 \quad \text{and} \quad \tilde{p}_e = T_e \tilde{n}_e. \quad (\text{A1})$$

Model equations are: The vorticity equation

$$\frac{\partial \nabla_{\perp}^2 \phi}{\partial t} + [\phi, \nabla_{\perp}^2 \phi] + \nabla_{\perp} \cdot [p_i, \nabla_{\perp} \phi] - \beta_e^{-1} \nabla_{\parallel} J_{\parallel} - (\mathbf{b} \times \boldsymbol{\kappa}) \cdot \nabla (P_e + p_i) - \mu_{\perp c} \nabla_{\perp}^4 \phi = S_{th1}, \quad (\text{A2})$$

the Ohm's law

$$\frac{\partial A_{\parallel}}{\partial t} + \nabla_{\parallel} (\phi - \tilde{p}_e) + \frac{1}{\xi} \left(\frac{\partial \tilde{J}_{\parallel}}{\partial t} + [\phi, \tilde{J}_{\parallel}] \right) + \eta_{\parallel} J_{\parallel} - \lambda_c \nabla_{\perp}^2 J_{\parallel} = S_{th2}, \quad (\text{A3})$$

the equation of parallel ion motion

$$\frac{\partial V_{\parallel}}{\partial t} + [\phi, V_{\parallel}] + \nabla_{\parallel} (P_e + p_i) - \mu_{\parallel c} \nabla_{\perp}^2 V_{\parallel} = S_{th3}, \quad (\text{A4})$$

the energy balance equation of electrons

$$\frac{\partial P_e}{\partial t} + [\phi, P_e] - (\mathbf{b} \times \boldsymbol{\kappa}) \cdot \nabla_{\perp} (P_e - \phi) + \nabla_{\parallel} P_e - \beta_e^{-1} \nabla_{\parallel}^2 J_{\parallel} - \chi_{e,c} \nabla_{\perp}^2 P_e = S_{th4}, \quad (\text{A5})$$

and the energy balance equation of ions

$$\frac{\partial p_i}{\partial t} + [\phi, p_i] + \beta \nabla_{\parallel} V_{\parallel} - \chi_c \nabla_{\perp}^2 p_i = S_{th5}. \quad (\text{A6})$$

In these equations, symbols denote

$$P_e = \frac{T_{e0}}{T_0} p_e, \quad J_{\parallel} = -\nabla_{\perp}^2 A_{\parallel}, \quad (\text{A7})$$

S_{th} stands for the thermodynamical excitations, and the bracket $[f, g]$ denotes the Poisson bracket,

$$[f, g] = (\nabla f \times \nabla g) \cdot \mathbf{b}, \quad (\text{A8})$$

Other notations are: $\mathbf{b} = \mathbf{B}_0/B_0$, $\Delta_\perp = \nabla_\perp^2$, $\kappa = \Omega' \hat{x}$ is the average curvature of the magnetic field, $1/\xi$ denotes the finite electron inertia, $1/\xi = (\delta/a)^2$, $v_{Ap} = B_0(2\mu_0 m_i n_i)^{-1/2} a R^{-1} q^{-1}$ the poloidal Alfvén velocity, a and R are minor and major radii of torus, m_i is the ion mass, and n_i is the ion density and the suffix 0 stands for the global parameters.

In studying the subcritical excitation, the electron inertia effect should be kept, but the classical resistivity is neglected for the simplicity of the argument. The interchange mode has a quasi-2 dimensional nature, $|\nabla_\parallel^2| \ll |\nabla_\perp^2|$; nevertheless, the existence of small but finite ∇_\parallel is essential. The product of two inhomogeneities

$$G_0 = \Omega' \frac{dp_0}{dx}, \quad (\text{A9})$$

denotes the driving parameter (i.e., one of the main control parameters in this system), being fixed in the evolution of fluctuating fields under the assumption of the time-space scale separation. Under this circumstance, the fluctuation part is separated as

$$\phi = \phi_0 + \tilde{\phi}, \quad J_\parallel = J_{\parallel,0} + \tilde{J}_\parallel, \quad V_\parallel = V_{\parallel,0} + \tilde{V}_\parallel, \quad p_e = p_{e,0} + \tilde{p}_e, \quad p_i = p_{i,0} + \tilde{p}_i \quad (\text{A10})$$

We consider the inhomogeneities of $\nabla\phi_0$, p_{e0} and p_{i0} . The influence of ∇V_\parallel on turbulence has been discussed, but is not investigated in this article. Keeping the relevant driving terms, the equations which govern the fluctuations are derived as

$$\begin{aligned} & \frac{\partial \nabla_\perp^2 \tilde{\phi}}{\partial t} + [\phi_0, \nabla_\perp^2 \tilde{\phi}] + \nabla_\perp \cdot [p_{i0}, \nabla_\perp \tilde{\phi}] - \beta_e^{-1} \nabla_\parallel \tilde{J}_\parallel - (\mathbf{b} \times \kappa) \cdot \nabla (\tilde{p}_e + \tilde{p}_i) - \mu_{\perp c} \nabla_\perp^4 \tilde{\phi} \\ & = -[\tilde{\phi}, \nabla_\perp^2 \tilde{\phi}] + S_{th1} \end{aligned} \quad (\text{A11})$$

$$(1 - \xi \nabla_\perp^2) \frac{\partial \tilde{J}_\parallel}{\partial t} + [\phi_0, \tilde{J}_\parallel] + \xi \nabla_\parallel (\tilde{\phi} - \tilde{p}_e) + \xi \eta_\parallel \tilde{J}_\parallel - \mu_{e,c} \nabla_\perp^2 \tilde{J}_\parallel = -[\phi, J_\parallel] + S_{th2} \quad (\text{A12})$$

$$\frac{\partial \tilde{V}_\parallel}{\partial t} + [\phi_0, \tilde{V}_\parallel] + \nabla_\parallel \tilde{p}_i - \mu_{\parallel c} \nabla_\perp^2 \tilde{V}_\parallel = -[\tilde{\phi}, \tilde{V}_\parallel] + S_{th3} \quad (\text{A13})$$

$$\frac{\partial \tilde{p}_e}{\partial t} + [\phi_0, \tilde{p}_e] - (\mathbf{b} \times \kappa) \cdot \nabla_\perp (\tilde{p}_e - \tilde{\phi}) + \nabla_\parallel \tilde{p}_e - \beta_e^{-1} \nabla_\parallel^2 \tilde{J}_\parallel - \chi_{c,e} \nabla_\perp^2 \tilde{p}_e$$

$$= -[\tilde{\Phi}, \tilde{P}_e] + S_{th4} \quad (A14)$$

$$\frac{\partial}{\partial t} \tilde{P}_i + [\Phi_0, \tilde{P}_i] + [\tilde{\Phi}, p_{i0}] + \beta \nabla_{\parallel} V_{\parallel} - \chi_c \nabla_{\perp}^2 \tilde{P}_i = -[\tilde{\Phi}, \tilde{P}_i] + S_{th5} \quad (A15)$$

In Eq.(A2), the term $[\nabla_{\perp} \tilde{P}_i, \nabla_{\perp} \tilde{\Phi}]$ is neglected. This term is known to enhance normal cascade. Other combinations of terms, $[\tilde{\Phi}, \nabla_{\perp}^2 \Phi_0]$ and $[\tilde{P}_i, \nabla_{\perp} \Phi_0]$, are also neglected, because the global parameters change much more slowly in comparison with fluctuations, and inequalities

$$|[\tilde{\Phi}, \nabla_{\perp}^2 \Phi_0]| \ll |[\Phi_0, \nabla_{\perp}^2 \tilde{\Phi}]| \quad \text{and} \quad |[\tilde{P}_i, \nabla_{\perp} \Phi_0]| \ll |[p_{i0}, \nabla_{\perp} \tilde{\Phi}]| \quad (A16)$$

usually hold.

In the presence of global radial electric field, the Poisson bracket $[\Phi_0, \tilde{X}]$ takes the form

$$[\Phi_0, \tilde{X}] = -E_{x,0} \frac{d}{dy} \tilde{X} = i V_{E \times B, y} k_y \tilde{X} \quad (A17)$$

where $V_{E \times B, y}$ is the y-component of the global $E \times B$ velocity. We introduce

$$\omega_E = V_{E \times B, y} k_y, \quad (A18)$$

and write

$$[\Phi_0, \tilde{X}] = i \omega_E \tilde{X}. \quad (A19)$$

Note that the spatially-inhomogeneous part of Eq.(A19) contributes to the evolution of the turbulence so long as the condition $V_{E \times B, y}^2 < v_{th,i}^2$ holds.

Linear part of the dynamical equations are rewritten as

$$\left(\frac{\partial}{\partial t} + i \omega_E + i k_y p'_{i0} \right) \tilde{\Phi} - \beta_e^{-1} \nabla_{\parallel} \nabla_{\perp}^{-2} \tilde{J}_{\parallel} - i k_y \Omega' \nabla_{\perp}^{-2} (\tilde{P}_e + \tilde{P}_i) - \mu_{\perp c} \nabla_{\perp}^2 \tilde{\Phi}$$

$$\left(\frac{\partial}{\partial t} + i \xi^{-1} \omega_E \right) \tilde{J}_{\parallel} + \xi \xi^{-1} \nabla_{\parallel} (\tilde{\Phi} - \tilde{P}_e) + \xi \xi^{-1} \eta_{\parallel} \tilde{J}_{\parallel} + \xi^{-1} \mu_{e,c} k_{\perp}^2 \tilde{J}_{\parallel}$$

$$\left(\frac{\partial}{\partial t} + i \omega_E \right) \partial \tilde{V}_{\parallel} + \nabla_{\parallel} \tilde{P}_i - \mu_{\parallel c} \nabla_{\perp}^2 \tilde{V}_{\parallel}$$

$$\left(\frac{\partial}{\partial t} + i\omega_E\right)\tilde{P}_e - i k_y P'_{e0} \tilde{\Phi} + i k_y \Omega' (\tilde{P}_e - \tilde{\Phi}) + \nabla_{\parallel} \tilde{P}_e - \beta_e^{-1} \nabla_{\parallel}^2 \tilde{J}_{\parallel} - \chi_{c,e} \nabla_{\perp}^2 \tilde{P}_e$$

$$\left(\frac{\partial}{\partial t} + i\omega_E\right)\tilde{P}_i - i k_y P'_{i0} \tilde{\Phi} + i\beta k_{\parallel} V_{\parallel} - \chi_c \nabla_{\perp}^2 \tilde{P}_i$$

with $\xi = 1 + \xi k_{\perp}^{-2}$. Equation (A11)-(A15) are rewritten as

$$\frac{\partial}{\partial t} f + \mathcal{L}^{(0)} f = \mathcal{N}(f, f) + \tilde{S}_{th} \quad (\text{A20})$$

with

$$\mathcal{L}^{(0)} = \begin{pmatrix} i\omega_E + i k_y P'_{i0} + \mu_{\perp} k_{\perp}^2 & i\beta_e^{-1} k_{\parallel} k_{\perp}^{-2} & 0 & i k_y \Omega' k_{\perp}^{-2} & i k_y \Omega' k_{\perp}^{-2} \\ i\xi \xi^{-1} k_{\parallel} & \xi^{-1} (i\omega_E + \xi \eta_{\parallel} + \mu_{c,e} k_{\perp}^2) & 0 & -i\xi \xi^{-1} k_{\parallel} & 0 \\ 0 & 0 & i\omega_E + \mu_{\parallel} k_{\perp}^2 & 0 & i k_{\parallel} \\ -i k_y P'_{e0} - i k_y \Omega' & -\beta_e^{-1} k_{\parallel}^2 & 0 & i\omega_E + i k_{\parallel} + i k_y \Omega' + \chi_{c,e} k_{\perp}^2 & 0 \\ -i k_y P'_{i0} & 0 & i\beta k_{\parallel} & 0 & i\omega_E + \chi_c k_{\perp}^2 \end{pmatrix} \quad (\text{A21})$$

and

$$\mathcal{N}(f, f) = - \begin{pmatrix} \nabla_{\perp}^{-2} [\phi, \nabla_{\perp}^2 \phi] \\ (1 - \xi \nabla_{\perp}^{-2})^{-1} [\phi, J_{\parallel}] \\ [\phi, V_{\parallel}] \\ [\phi, P_e] \\ [\phi, P_i] \end{pmatrix}, \quad (\text{A22})$$

for

$$f = \begin{pmatrix} \phi \\ J_{\parallel} \\ V_{\parallel} \\ P_e \\ P_i \end{pmatrix}. \quad (\text{A23})$$

Appendix B: Separation of Components

Nonlinear interaction term is separated as

$$\mathcal{N}(f, f) = \mathcal{P}^l \mathcal{N}(f, f) + \mathcal{P}^h \mathcal{N}(f, f) \quad (\text{B1})$$

where \mathcal{P}^l and \mathcal{P}^h are projection operators which select the semi-micro and micro components, respectively. Fluctuation fields are decomposed as

$$f = \mathcal{P}^l f + \mathcal{P}^h f \equiv f^l + f^h \quad (\text{B2})$$

and the nonlinear terms are formally rewritten as

$$\mathcal{N}(f, f) = \mathcal{N}(\mathcal{P}^l f + \mathcal{P}^h f, \mathcal{P}^l f + \mathcal{P}^h f). \quad (\text{B3})$$

The term $\mathcal{N}(f, f)$ has a quadratic form of the fluctuation fields, and one has

$$\mathcal{N}(f, f) = \mathcal{N}(\mathcal{P}^l f, \mathcal{P}^l f) + \mathcal{N}(\mathcal{P}^l f, \mathcal{P}^h f) + \mathcal{N}(\mathcal{P}^h f, \mathcal{P}^l f) + \mathcal{N}(\mathcal{P}^h f, \mathcal{P}^h f) \quad (\text{B4})$$

The term $\mathcal{N}(\mathcal{P}^l f, \mathcal{P}^l f)$ provides semi-micro components, and the terms $\mathcal{N}(\mathcal{P}^l f, \mathcal{P}^h f)$ and $\mathcal{N}(\mathcal{P}^h f, \mathcal{P}^l f)$ contribute to the micro components. The last term of Eq.(B4) yields both the semi-micro and micro components. Considering these facts, the semi-micro and micro components in nonlinear terms are given as

$$\mathcal{P}^l \mathcal{N}(f, f) = \mathcal{N}(\mathcal{P}^l f, \mathcal{P}^l f) + \mathcal{P}^l \mathcal{N}(\mathcal{P}^h f, \mathcal{P}^h f) \quad (\text{B5})$$

and

$$\mathcal{P}^h \mathcal{N}(f, f) = \mathcal{N}(\mathcal{P}^h f, \mathcal{P}^l f) + \mathcal{N}(\mathcal{P}^l f, \mathcal{P}^h f) + \mathcal{P}^h \mathcal{N}(\mathcal{P}^h f, \mathcal{P}^h f) \quad (\text{B6})$$

The self interaction terms are expressed in terms of the drag and noise (see I-V), and one has

$$\mathcal{P}^l \mathcal{N}(\mathcal{P}^l f, \mathcal{P}^l f) = -\Gamma_{(l)}^l f^l + \tilde{S}_{(l)}^l \quad (\text{B7})$$

and

$$\mathcal{P}^h \mathcal{N}(\mathcal{P}^h f, \mathcal{P}^h f) = -\Gamma_{(h)}^h f^h + \tilde{S}_{(h)}^h \quad (\text{B8})$$

for semi-micro mode. In this expression, the subscripts (l) and (h) denote that the interactions are driven by semi-micro and micro modes, respectively. Combining Eqs.(B7) and (B8), we have the nonlinear term for semi-micro mode as

$$\mathcal{P}^l \mathcal{N}(f, f) = -\left(\Gamma_{(l)}^l + \Gamma_{(h)}^l\right) f^l + \tilde{S}_{(l)}^l + \tilde{S}_{(h)}^l. \quad (\text{B9})$$

For micro mode, one has the expression for self-interaction term as

$$\mathcal{P}^h \mathcal{N}(\mathcal{P}^h f, \mathcal{P}^h f) = -\Gamma_{(h)}^h f^h + \tilde{S}_{(h)}^h. \quad (\text{B10})$$

There appear cross terms (the first and second terms in the right hand side of Eq.(B6). The cross terms $\mathcal{N}(\mathcal{P}^l f, \mathcal{P}^h f)$ and $\mathcal{N}(\mathcal{P}^h f, \mathcal{P}^l f)$ are linear with respect to $\mathcal{P}^h f$. The spatial scale of modification of plasma parameters by semi-micro mode, $\mathcal{P}^l f$, is much longer than the characteristic length of the micro mode. Owing to this consideration, the cross term is interpreted as a modification of the driving parameters for the dynamics of micro mode. We therefore write the cross terms as 'drive' terms, and use a symbol

$$\mathcal{D}_{(l)}^h f^h = \mathcal{N}(\mathcal{P}^h f, \mathcal{P}^l f) + \mathcal{N}(\mathcal{P}^l f, \mathcal{P}^h f). \quad (\text{B11})$$

Abbreviations

$$f^l = \mathcal{P}^l f \quad (\text{B12})$$

$$f^h = \mathcal{P}^h f \quad (\text{B13})$$

are used.

The driving term Eq.(B11) is explicitly given for the case of the five-field model in Appendix A. The cross terms in the nonlinear terms are written as

$$\mathcal{D}_{(l)}^h f^h = - \left(\begin{array}{l} \left(ik_y \frac{\partial}{\partial x} \tilde{\Phi}^l - ik_x \frac{\partial}{\partial y} \tilde{\Phi}^l \right) \tilde{\Phi}_k^h \\ \xi^{-1} \left\{ \left(ik_y \frac{\partial}{\partial x} \tilde{\Phi}^l - ik_x \frac{\partial}{\partial y} \tilde{\Phi}^l \right) \tilde{J}_{\parallel, k}^h - \left(ik_y \frac{\partial}{\partial x} \tilde{J}_{\parallel}^l - ik_x \frac{\partial}{\partial y} \tilde{J}_{\parallel}^l \right) \tilde{\Phi}_{\parallel, k}^h \right\} \\ \left(ik_y \frac{\partial}{\partial x} \tilde{\Phi}^l - ik_x \frac{\partial}{\partial y} \tilde{\Phi}^l \right) \tilde{V}_{\parallel, k}^h - \left(ik_y \frac{\partial}{\partial x} \tilde{V}_{\parallel}^l - ik_x \frac{\partial}{\partial y} \tilde{V}_{\parallel}^l \right) \tilde{\Phi}_k^h \\ \left(ik_y \frac{\partial}{\partial x} \tilde{\Phi}^l - ik_x \frac{\partial}{\partial y} \tilde{\Phi}^l \right) \tilde{P}_{ek}^h - \left(ik_y \frac{\partial}{\partial x} \tilde{P}_e^l - ik_x \frac{\partial}{\partial y} \tilde{P}_e^l \right) \tilde{\Phi}_k^h \\ \left(ik_y \frac{\partial}{\partial x} \tilde{\Phi}^l - ik_x \frac{\partial}{\partial y} \tilde{\Phi}^l \right) \tilde{P}_{ik}^h - \left(ik_y \frac{\partial}{\partial x} \tilde{P}_i^l - ik_x \frac{\partial}{\partial y} \tilde{P}_i^l \right) \tilde{\Phi}_k^h \end{array} \right) \quad (\text{B14})$$

with $\xi = 1 + \xi k_{\perp}^{-2}$. The operator that shows the nonlinear drive is given as

$$\mathcal{D}_{(l)}^h = - \left(\begin{array}{ccccc} i \omega_{E(l)} & 0 & 0 & 0 & 0 \\ i \xi^{-1} \omega_{2(l)} & i \xi^{-1} \omega_{E(l)} & 0 & 0 & 0 \\ i \omega_{3(l)} & 0 & i \omega_{E(l)} & 0 & 0 \\ i \omega_{4(l)} & 0 & 0 & i \omega_{E(l)} & 0 \\ i \omega_{5(l)} & 0 & 0 & 0 & i \omega_{E(l)} \end{array} \right) \quad (\text{B15})$$

where

$$\omega_{E(l)} = k_y \frac{\partial}{\partial x} \tilde{\Phi}^l - k_x \frac{\partial}{\partial y} \tilde{\Phi}^l \quad (\text{B16})$$

is the Doppler shift owing to the $E \times B$ velocity associated with the semi-micro mode, and

$$\omega_{j(l)} = -k_y \frac{\partial}{\partial x} \tilde{f}_j^l + k_x \frac{\partial}{\partial y} \tilde{f}_j^l \quad (j = 2 - 5) \quad (\text{B17})$$

represents the modification of plasma parameters by the semi-micro mode. A combination of terms $[\tilde{\Phi}^h, \nabla_{\perp}^2 \tilde{\Phi}^l]$ is neglected, because the inequality

$$\left| [\tilde{\Phi}^h, \nabla_{\perp}^2 \tilde{\Phi}^l] \right| \ll \left| [\tilde{\Phi}^l, \nabla_{\perp}^2 \tilde{\Phi}^h] \right| \quad (\text{B18})$$

holds.

Appendix C: Average Model Estimate

Spectrum averages appear in renormalization relations and extended fluctuation dissipation theorems. Order of magnitude estimate which is based on dimensional arguments is made assuming that summations converge. In Eq.(57), the summation is estimated as

$$\sum_k^{micro\ modes} M_{i, kk'q} M_{i, qkk'}^* \left| \tilde{f}_{i, k'}^2 \right| \rightarrow (k_0^h)^4 I_i^h, \quad (C1)$$

where the total fluctuation level for micro mode is given by

$$I_j^h = \sum_k I_{j, k}^h = \sum_k \left\langle f_{j, k}^{h*} f_{j, k}^h \right\rangle. \quad (C2)$$

With this approximation, Eq.(59) is order estimated as

$$\gamma_i^h = \frac{(k_0^h)^4}{\gamma_i^{h*} + \gamma_{ic}^h} I_i^h \quad (C3a)$$

or

$$\gamma_i^h (\gamma_i^{h*} + \gamma_{ic}^h) = (k_0^h)^4 I_i^h, \quad (C3b)$$

where γ_i^h is the characteristic eddy-damping rate of the micro mode, and k_0^h is the characteristic wave number of the micro mode.

In Eqs.(59) and (60), the summations are estimated as

$$- \sum_p^{semi-micro\ modes} M_{i, kpq} M_{i, qkp}^* \gamma_{i, k}^{*-1} \left| \tilde{f}_{i, p}^2 \right| \rightarrow \gamma_i^{l* -1} (k_0^l)^4 I_i^l \quad (C4)$$

and

$$- \sum_p^{micro\ modes} M_{i, kpq} M_{i, qkp}^* \gamma_{i, k}^{*-1} \left| \tilde{f}_{i, p}^2 \right| \rightarrow \gamma_i^{h* -1} (k_0^l)^2 (k_0^h)^2 I_i^h \quad (C5)$$

where the total fluctuation level for semi-micro mode is given by

$$I_j^l = \sum_k I_{j, k}^l = \sum_k \left\langle f_{j, k}^{l*} f_{j, k}^l \right\rangle. \quad (C6)$$

By use of Eqs.(C4) and (C5), one has

$$\gamma_i^l = \frac{(k_0^l)^4}{\gamma_i^{l*} + \gamma_{ic}^l} I_i^l + \frac{(k_0^l)^2 (k_0^h)^2}{\gamma_i^{h*} + \gamma_{ic}^h} I_i^h \quad (C7a)$$

or

$$\gamma_i^l (\gamma_i^{l*} + \gamma_{ic}^l) = (k_0^l)^4 I_i^l + (k_0^l)^2 (k_0^h)^2 \frac{\gamma_i^{l*} + \gamma_{ic}^l}{\gamma_i^{h*} + \gamma_{ic}^h} I_i^h, \quad (C7b)$$

where γ_i^l is the characteristic eddy-damping time of the semi-micro mode, and k_0^l is the characteristic wave number of the semi-micro mode.

Equations (C3) and (C7) are the relations between the total fluctuation level and (spectrum-averaged) damping rates and wave numbers.

Similar arguments are possible for the extended-fluctuation dissipation theorem, Eq.(78). It is approximated as

$$\Re(\lambda_1^l) I_1^l = \frac{C_0^l}{2} \gamma_v^l I_1^l + \frac{\hat{C}_0^h}{2} \gamma_v^h \left(\frac{k_0^l}{k_0^h} \right)^4 I_1^h \quad (C8)$$

where λ_1^l is the characteristic (spectrum-averaged) eigenvalue for the nonlinear dispersion relation.

References

- 1) Yoshizawa A, Itoh S-I, Itoh K, Yokoi N 2001 Plasma Phys. Contr. Fusion **43** R1.
- 2) Horton C W 1999 Rev. Mod. Phys. **71** 735
- 3) Krommes J A 2001 "Fundamental statistical theories of plasma turbulence in magnetic fields" Phys. Reports in press.
- 4) Connor J W 1988 Plasma Phys. Contr. Fusion **30** 619.
- 5) Itoh K, Itoh S-I and Fukuyama A 1999 *Transport and Structural Formation in Plasmas* (IOP, Bristol)
- 6) Yoshizawa A 1998 *Hydrodynamic and Magnetohydrodynamic Turbulent Flows: Modeling and Statistical Theory* (Kluwer, Dordrecht).
- 7) Itoh S-I and Itoh K 1998 "Statistical Theory of Subcritically-Excited Strong Turbulence in Inhomogeneous Plasmas" Research Report IPP III/234 (Max-Planck-Institut für Plasmaphysik).
- 8) Itoh S-I and Itoh K 1999 J. Phys. Soc. Jpn. **68** 1891.
- 9) Itoh S-I and Itoh K 1999 J. Phys. Soc. Jpn. **68** 2611.
- 10) Itoh S-I and Itoh K 2000 J. Phys. Soc. Jpn. **69** 408.
- 11) Itoh S-I and Itoh K 2000 J. Phys. Soc. Jpn. **69** 427.
- 12) Itoh S-I and Itoh K 2000 J. Phys. Soc. Jpn. **69** 3253.
- 13) Kraichnan R H 1959 J. Fluid Mech. **5** 497.
- 14) Bowman J C, Krommes J A, Ottaviani M 1993 Phys. Fluids B **5** 3558.
- 15) Krommes J A 1996 Phys. Rev. E **53** 4865.
- 16) See, e.g., Kubo R, Toda M, Hashitsume N 1985 : *Statistical Physics II* (Springer, Berlin).
- 17) Prigogine I 1961 *Introduction to Thermodynamics of Irreversible Processes*, 2nd ed. (Interscience Publishers, New York).
- 18) Fowler R H 1936 *Statistical Mechanics* (second ed., Cambridge) Chap.18.
- 19) Itoh S-I, Itoh K, Fukuyama A, Miura Y 1991 Phys. Rev. Lett. **67** 2485.
- 20) Diamond P H, et al. 1997 Phys. Rev. Lett. **78** 1472.
- 21) Smolyakov A I and Diamond P H 1999 Phys. Plasmas **6** 4410.
- 22) Drake J F, Zeiler A, Biskamp D 1995 Phys. Rev. Lett. **75** 4222.
- 23) Krommes J A and Kim C-B 2000 Phys. Rev. E. **62** 8508.
- 24) Yagi M 2000 "Study on Nonlocal Transport Based on Transport-MHD Model" presented at US-JAPAN Workshop on "Self-organization" (NIFS, Dec.).
- 25) Lopes Cardozo N 1995 Plasma Phys. Contr. Fusion **37** 799;
Callen J D and Kissik M W 1997 Plasma Phys. Contr. Fusion **39** B173;
Stroth U 1998 Plasma Phys. Contr. Fusion **40** 9.
- 26) See reviews, e.g., Itoh S-I *et al.*: J. Nucl. Materials **220-222** 117,
Staebler G M 1998 Plasma Phys. Contr. Fusion **40** 569,

- Wakatani M 1998 Plasma Phys. Contr. Fusion **40** 597.
- 27) Yagi M 1989 PhD thesis; *Study of anomalous transport based on drift and resistive instabilities in Heliotron/torsatron configuration* (Kyoto University).
 - 28) Itoh S-I and Itoh K: J. Phys. Soc. Jpn. **59** (1990) 3815.
 - 29) Shaing K C, Crume E C Jr., Houlberg W A 1990 Phys. Fluids B **2** 1492.
 - 30) Biglari H, Diamond P H, Terry P W 1990 Phys. Fluids B **2** 1.
 - 31) Zhang Y Z and Mahajan S M 1992 Phys. Fluids B **4** 1385.
 - 32) Itoh S-I, Itoh K, Fukuyama A, Yagi M 1994 Phys. Rev. Lett. **72** 1200.
 - 33) Terry P W 2000 Rev. Mod. Phys. **72** 109.
 - 34) Kraichnan R H 1970 J. Fluid Mech. **41** 189.
 - 35) Krommes J A 1999 Plasma Phys. Contr. Fusion **41** A641.
 - 36) Hamaguchi S and Horton C W 1992 Phys. Fluids B **4** 319.
 - 37) Itoh K, Itoh S-I, Fukuyama A 1992 Phys. Rev. Lett. **69** 1050;
Itoh K, Fukuyama A, Itoh S-I, Yagi M 1995 Plasma Phys. Control. Fusion **37** 707.
 - 38) Uchida M, Fukuyama A, Itoh K, Itoh S-I, Yagi M 1998 in Proc. 9th International Toki Conference (National Inst. Fusion Science, 1998).
 - 39) Diamond P H and Carreras B A 1987 *Comments Plasma Phys. Contr. Fusion* **10** 271.
 - 40) Itoh K, Itoh S-I, Yagi M, Fukuyama A, Azumi M 1993 *Phys. Fluids* **B5** 3299.
 - 41) Hahn T S, Burrell K H, Lin Z, Nazikian R, Synakowski E J 2000 Plasma Phys. Contr. Fusion **42** A205.
 - 42) Krommes J A 2000 Phys. Plasmas **7** 1148
 - 43) Itoh K, Itoh S-I, Yagi M, Fukuyama A 1996 Plasma Phys. Control. Fusion **38** 2079.
 - 44) Parail V V 1997 Nucl. Fusion **37** 481.
 - 45) Iwasaki T, et al. 1999 J. Phys. Soc. Jpn. **68** 478.
 - 46) Iwasaki T, et al. 1999 Nucl. Fusion **39** 2127.
 - 47) Itoh K, Fukuyama A, Itoh S-I 1993 Plasma Phys. Contr. Fusion **35** 723.
 - 48) Kubo R 1962 J. Phys. Soc. Jpn. **17** 1100.

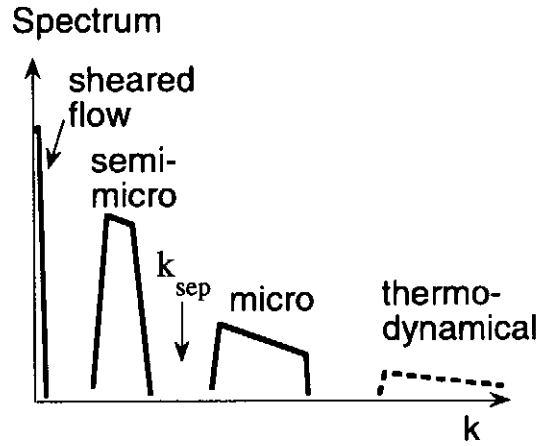


Fig.1: Schematic distribution of symmetry-breaking structures in the wave-number space: Sheared global flow, semi-micro mode fluctuations, micro-mode fluctuations and thermodynamical fluctuations.

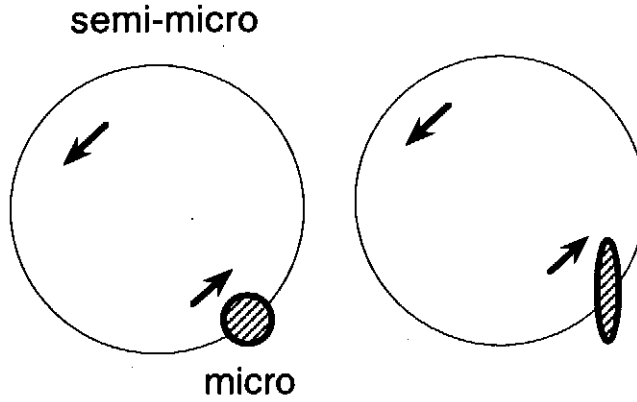


Fig.2: Stretching of the micro mode by the semi-micro mode.

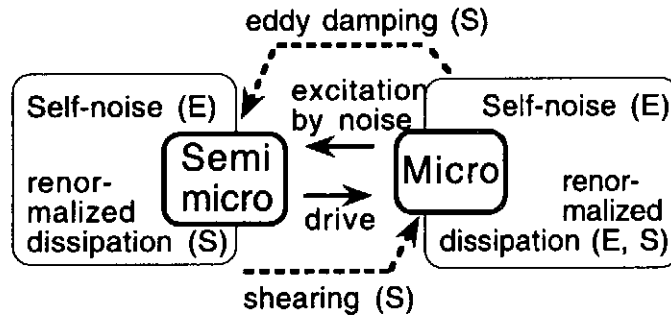
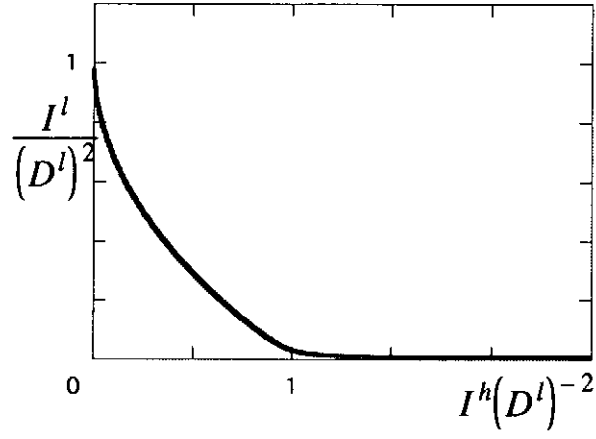


Fig.3: Mutual nonlinear interactions between the semi-micro mode and micro mode. Symbol (E) and (S) denote 'excitation' and 'suppressing effect' respectively.

(a)



(b)

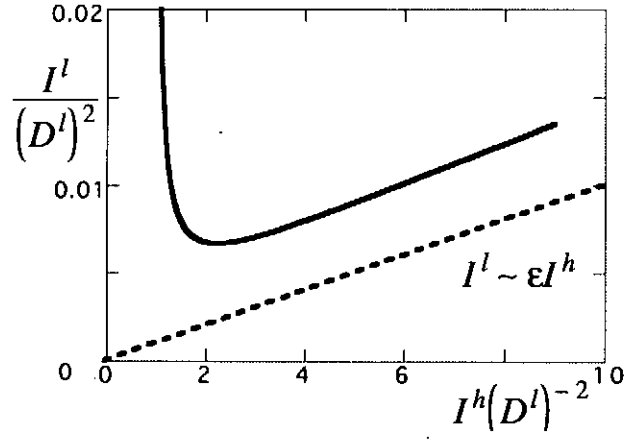
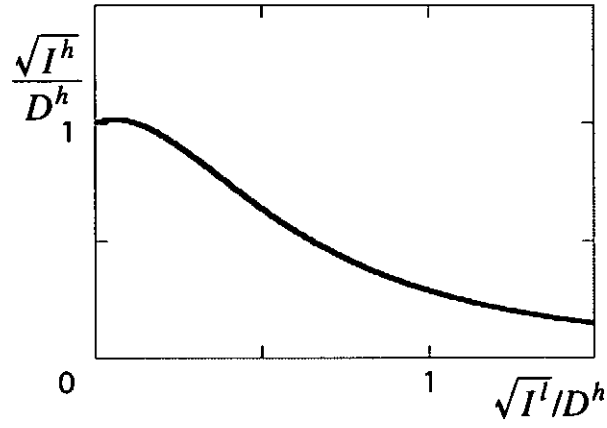


Fig.4 Fluctuation level of the semi-micro mode I^l as a function of the fluctuation level of micro mode I^h for fixed value ϵ . Coordinates are normalized to D^l . An expanded view for the small values of I^l is given in (b). Parameter is set as $\epsilon = 10^{-3}$ for illustration.

(a)



(b)

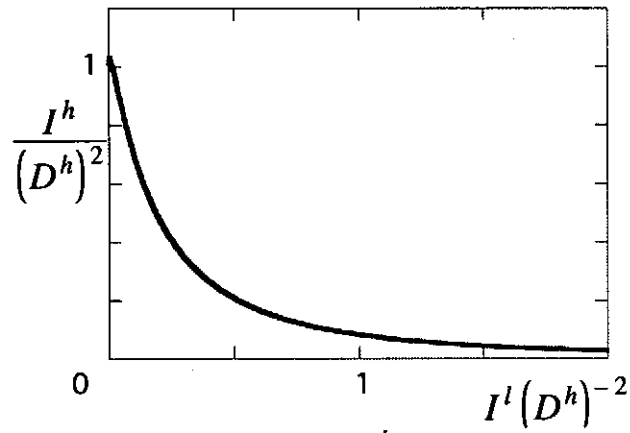


Fig.5 Fluctuation level of micro mode I^h as a function of the level of semi-micro mode I^l ; in terms of fluctuation amplitude $\sqrt{I^h}$ (a) and fluctuation level I^h (b), respectively. Other parameter is chosen as $\sqrt{I_{eff}} = D^h/2$.

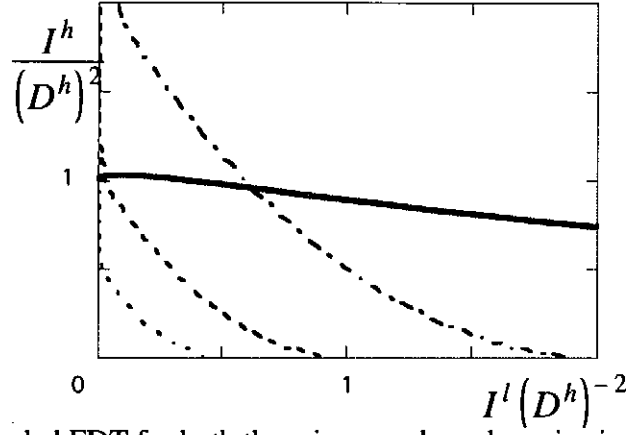


Fig.6 Extended FDT for both the micro mode and semi-micro mode must be satisfied simultaneously. Extended FDT for micro mode (the case where nonlinear effect of the semi-micro mode is weak, $\sqrt{I_{eff}} = 2.5 D^h$, solid line) and that for semi-micro mode for various values of the drive term D^l ($D^l = D^h/\sqrt{2}$ for dotted line, $D^l = D^h$ for dashed line, and $D^l = \sqrt{2}D^h$ for dash-dotted line) are shown. The cross point represents the self-consistent solution.

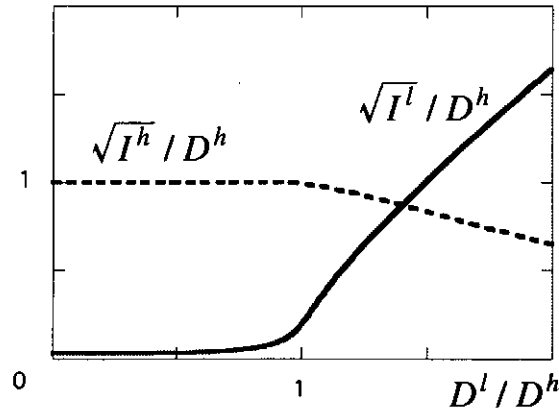


Fig.7 Fluctuation amplitude for semi-micro mode $\sqrt{I^l}$ (solid line) and that for micro mode $\sqrt{I^h}$ (dashed line) as a function of the driving rate of the semi-micro mode D^l . The driving rate for the micro mode, D^h , is fixed as $D^h = \sqrt{0.3 I_{eff}}$.

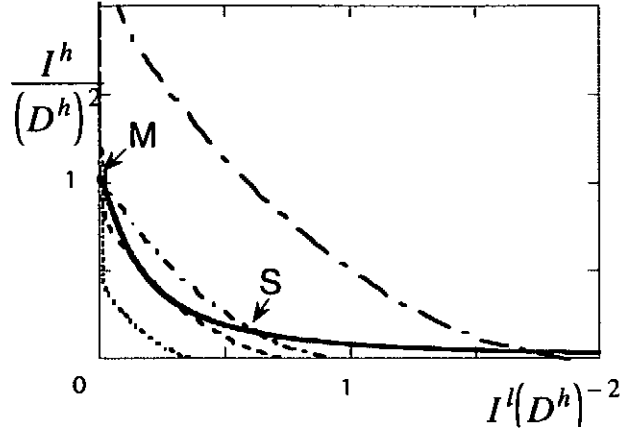


Fig.8 Extended FDT for both the micro mode (solid line) and semi-micro mode ($D^l \simeq 0.6D^h$ for dotted line, $D^l \simeq 0.74D^h$ for dashed line, $D^l \simeq D^h$ for short broken line, and $D^l = \sqrt{2}D^h$ for long broken line) in the case where suppression of micro mode by semi-micro mode is efficient $\sqrt{I_{eff}} = 0.5 D^h$. Multiple solutions 'S' and 'M' can exist for the intermediate strength of the drive rate of semi-micro mode D^l . Symbol 'S' denotes the solution where semi-micro mode turbulence is excited. The solution 'M' indicates the one where semi-micro mode is quenched.

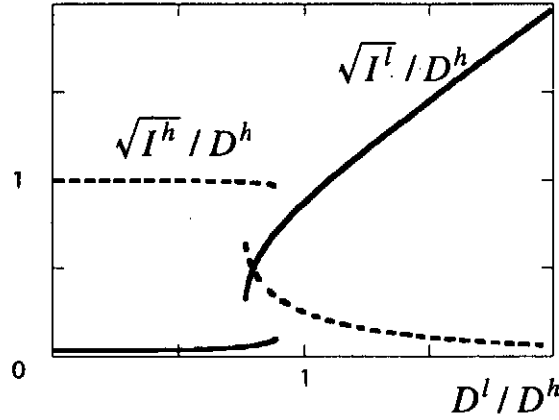


Fig.9 Fluctuation level for semi-micro mode I^l (solid line) and that for micro mode I^h (dashed line) as a function of the driving rate of the semi-micro mode D^l . (For the case of Fig.8, i.e., $\sqrt{I_{eff}} = 0.5 D^h$.) The driving rate for the micro mode D^h is fixed. For the intermediate value of D^l , multiple solutions are allowed and hard transition takes place at critical values of D^l .

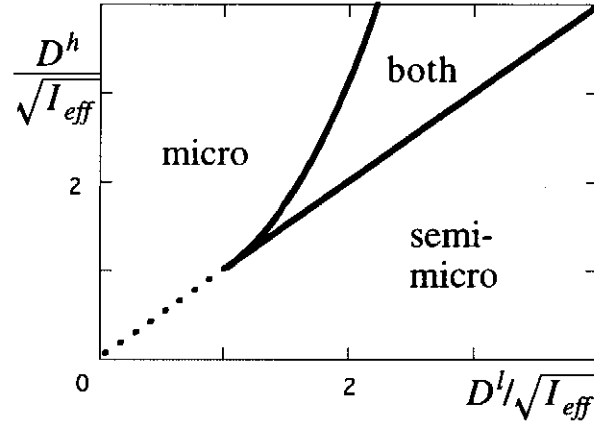


Fig.10 Phase diagram on the plane of global parameters, being represented by D^l and D^h . Coordinates are normalized to $\sqrt{I_{eff}}$. A cusp type catastrophe is obtained. In the region of "micro", the semi-micro mode level is quenched and is very low. In the region of "semi-micro", the micro mode coexists but is suppressed.

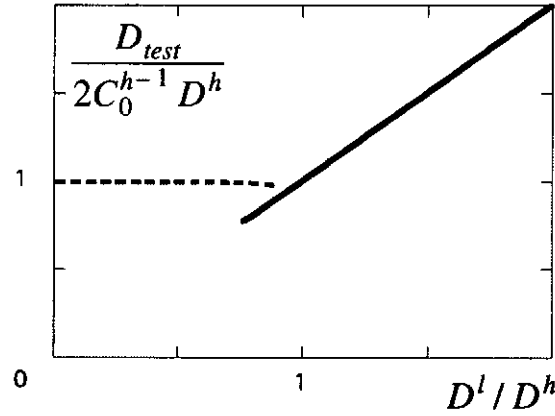


Fig.11(a) Test particle diffusion coefficient D_{test} as a function of the drive for the semi-micro mode D^l . The case of $C_0^h = C_0^l$ is shown for illustration. Horizontal axis is normalized to D^h , and vertical axis is normalized to $2D^h/C_0^h$. The case of hard transition for the parameters of Fig.9 is given in (a); solid line is for the branch 'S' and the dashed line is for the branch 'M'.

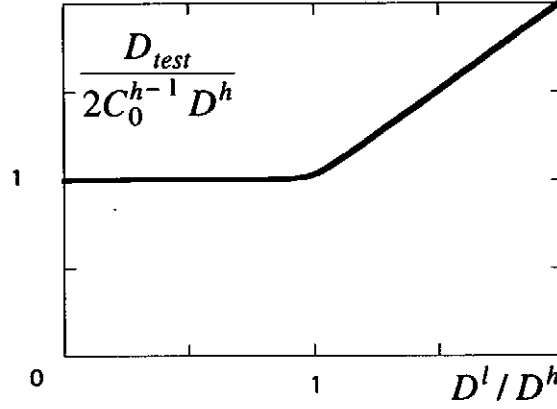


Fig.11(b) Test particle diffusion coefficient D_{test} as a function of the drive for the semi-micro mode D^l . The case of $C_0^h = C_0^l$ is shown for illustration. Horizontal axis is normalized to D^h , and vertical axis is normalized to $2D^h/C_0^h$. The case of soft transition for the parameters of Fig.7 is given in (b).

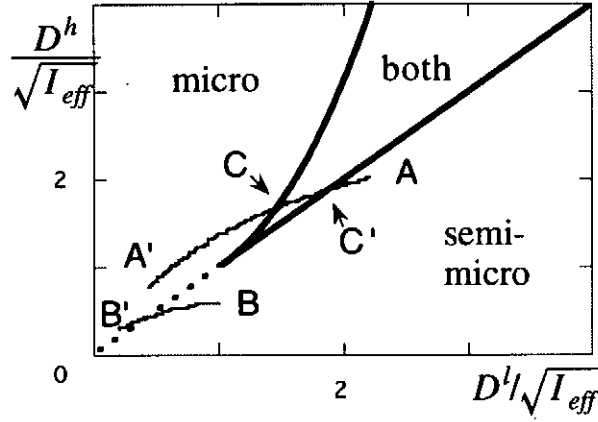
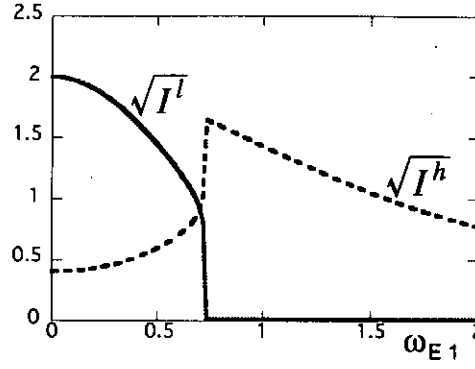
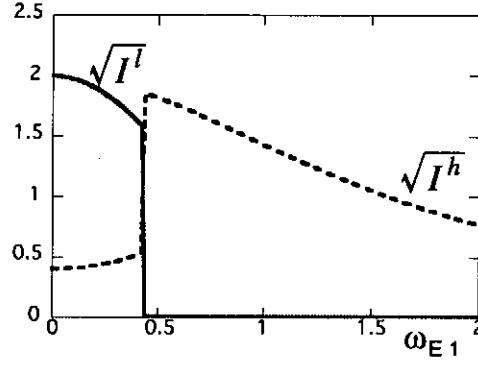


Fig.12 Trajectory of the driving parameters $D^l(\omega_{E1}^l)$ and $D^h(\omega_{E1}^h)$ as the global electric field shear increases. ω_{E1} changes from $\omega_{E1}/\omega_{Ec}^l = 0$ to $\omega_{E1}/\omega_{Ec}^l = 2$. (Normalization is the same as in Fig.10.) States A and B (in the absence of the electric field shear) is chosen in the branch where semi-micro fluctuations dominates. A hard transition takes place at C and the back-transition at C'. $D^l(0) = 2.2\sqrt{I_{eff}}$, $D^h(0) = 2\sqrt{I_{eff}}$ and $\omega_{Ec}^l = \sqrt{0.4} \omega_{Ec}^h$ for (A-A'); $D^l(0) = \sqrt{I_{eff}}$, $D^h(0) = 0.6\sqrt{I_{eff}}$ and $\omega_{Ec}^l = \sqrt{0.3} \omega_{Ec}^h$ for (B-B').

(a)



(b)



(c)

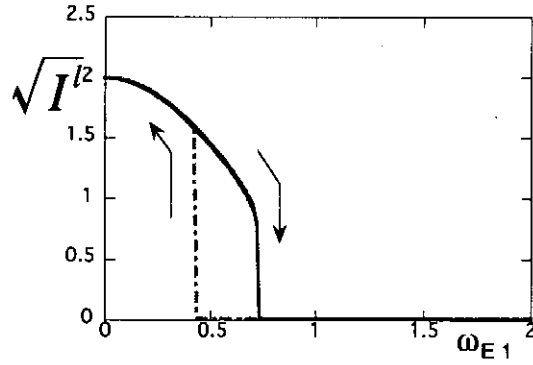


Fig.13 Fluctuation amplitude $\sqrt{I^l}$ (solid line) and $\sqrt{I^h}$ (dashed line) as a function of the shear of global $E \times B$ velocity $\omega_{E1}/\omega_{Ec}^l$. ω_{E1} changes from $\omega_{E1}/\omega_{Ec}^l = 0$ to $\omega_{E1}/\omega_{Ec}^l = 2$. ($\sqrt{I^l}$ and $\sqrt{I^h}$ are normalized to $\sqrt{I_{eff}}$.) The case of hard transition. Parameters are: $D^l(0) = 2.2\sqrt{I_{eff}}$, $D^h(0) = 2\sqrt{I_{eff}}$ and $\omega_{Ec}^l = \sqrt{0.4} \omega_{Ec}^h$. The situation where ω_{E1} is increasing is shown in (a) and that ω_{E1} is decreasing is shown in (b). Hysteresis of the semi-micro mode amplitude is illustrated in (c).

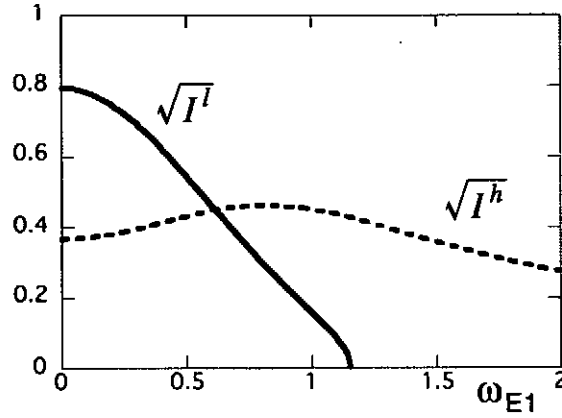


Fig.14 Fluctuation amplitude $\sqrt{I^l}$ (solid line) and $\sqrt{I^h}$ (dashed line) as a function of the shear of global $E \times B$ velocity. ω_{E1} changes from $\omega_{E1}/\omega_{Ec}^l = 0$ to $\omega_{E1}/\omega_{Ec}^l = 2$. ($\sqrt{I^l}$ and $\sqrt{I^h}$ are normalized to $\sqrt{I_{eff}}$.) The case of the soft transition: $D^l(0) = \sqrt{I_{eff}}$, $D^h(0) = 0.6\sqrt{I_{eff}}$ and $\omega_{Ec}^l = \sqrt{0.3} \omega_{Ec}^h$.

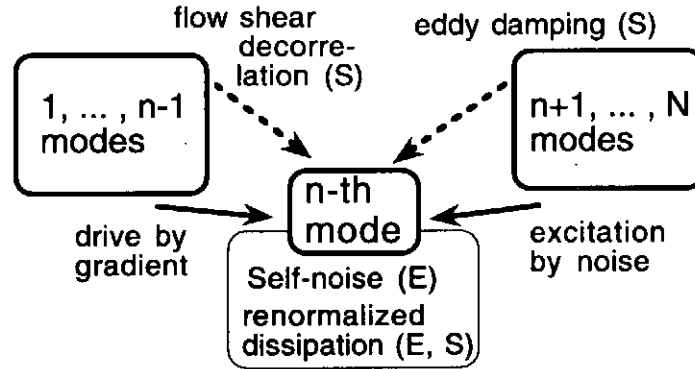


Fig.15 Hierarchical structure in mutual nonlinear interactions between the n -th mode and the smaller scale modes ($n' = n + 1, \dots, N$) and the larger scale modes ($n' = 1, \dots, n - 1$). Symbol (E) and (S) denote 'excitation' and 'suppressing effect' respectively.

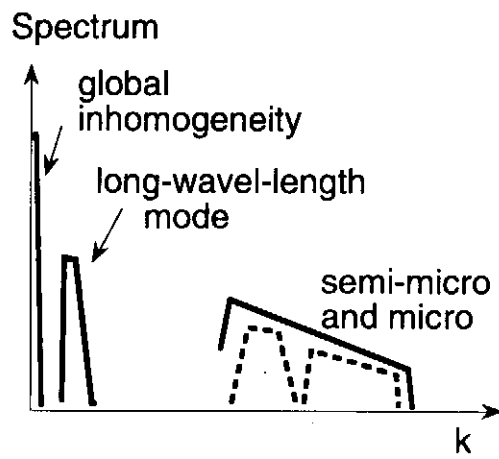


Fig.16 Long-wave-length mode is excited by microscopic modes (semi-micro mode and micro mode) in inhomogeneous plasmas.

Recent Issues of NIFS Series

- NIFS-677 S. Satake, H. Sugama, M. Okamoto and M. Wakatani,
Classification of Particle Orbits near the Magnetic Axis in a Tokamak by Using Constants of Motion: Jan. 2001
- NIFS-678 M. Tanaka and A. Yu Grosberg,
Giant Charge Inversion of a Macroion Due to Multivalent Counterions and Monovalent Coions: Molecular Dynamics Studyn: Jan. 2001
- NIFS-679 K. Akaishi, M. Nakasuga, H. Suzuki, M. Iima, N. Suzuki, A. Komori, O. Motojima and Vacuum Engineering Group,
Simulation by a Diffusion Model for the Variation of Hydrogen Pressure with Time between Hydrogen Discharge Shots in LHD: Feb. 2001
- NIFS-680 A. Yoshizawa, N. Yokoi, S. Nisizima, S.-I. Itoh and K. Itoh
Variational Approach to a Turbulent Swirling Pipe Flow with the Aid of Helicity: Feb. 2001
- NIFS-681 Alexander.A.Shishkin
Estafette of Drift Resonances, Stochasticity and Control of Particle Motion in a Toroidal Magnetic Trap: Feb. 2001
- NIFS-682 H. Momota and G.H. Miley,
Virtual Cathode in a Spherical Inertial Electrostatic Confinement Device: Feb. 2001
- NIFS-683 K. Saito, R. Kumazawa, T. Mutoh, T. Seki, T. Watari, Y. Torii, D.A. Hartmann, Y. Zhao, A. Fukuyama, F. Shimpo, G. Nomura, M. Yokota, M. Sasao, M. Isobe, M. Osakabe, T. Ozaki, K. Narihara, Y. Nagayama, S. Inagaki, K. Itoh, S. Morita, A.V. Krasilnikov, K. Ohkubo, M. Sato, S. Kubo, T. Shimoizuma, H. Idei, Y. Yoshimura, O. Kaneko, Y. Takeiri, Y. Oka, K. Tsumori, K. Ikeda, A. Komori, H. Yamada, H. Funaba, K.Y. Watanabe, S. Sakakibara, M. Shoji, R. Sakamoto, J. Miyazawa, K. Tanaka, B.J. Peterson, N. Ashikawa, S. Murakami, T. Minami, S. Ohakachi, S. Yamamoto, S. Kado, H. Sasao, H. Suzuki, K. Kawahata, P. deVries, M. Emoto, H. Nakanishi, T. Kobuchi, N. Inoue, N. Ohyabu, Y. Nakamura, S. Masuzaki, S. Muto, K. Sato, T. Morisaki, M. Yokoyama, T. Watanabe, M. Goto, I. Yamada, K. Ida T. Tokuzawa, N. Noda, S. Yamaguchi, K. Akaishi, A. Sagara, K. Toi, K. Nishimura, K. Yamazaki, S. Sudo Y. Hamada, O. Motojima, M. Fujiwara,
Ion and Electron Heating in ICRF Heating Experiments on LHD: Mar. 2001
- NIFS-684 S. Kida and S. Goto,
Line Statistics:Stretching Rate of Passive Lines in Turbulence: Mar. 2001
- NIFS-685 R. Tanaka, T. Nakamura and T. Yabe,
Exactly Conservative Semi-Lagrangian Scheme (CIP-CSL) in One-Dimension : Mar. 2001
- NIFS-686 S. Toda and K. Itoh,
Analysis of Structure and Transition of Radial Electric Field in Helical Systems : Mar. 2001
- NIFS-687 T. Kuroda and H. Sugama,
Effects of Multiple-Helicity Fields on Ion Temperature Gradient Modes: Apr. 2001
- NIFS-688 M. Tanaka,
The Origins of Electrical Resistivity in Magnetic Reconnection: Studies by 2D and 3D Macro Particle Simulations: Apr. 2001
- NIFS-689 A. Maluckov, N. Nakajima, M. Okamoto, S. Murakami and R. Kanno,
Statistical Properties of the Neoclassical Radial Diffusion in a Tokamak Equilibrium: Apr. 2001
- NIFS-690 Y. Matsumoto, T. Nagaura, Y. Itoh, S.-I. Oikawa and T. Watanabe,
LHD Type Proton-Boron Reactor and the Control of its Peripheral Potential Structure: Apr. 2001
- NIFS-691 A. Yoshizawa, S.-I. Itoh, K. Itoh and N. Yokoi,
Turbulence Theories and Modelling of Fluids and Plasmas: Apr. 2001
- NIFS-692 K. Ichiguchi, T. Nishimura, N. Nakajima, M. Okamoto, S.-i. Oikawa, M. Itagaki,
Effects of Net Toroidal Current Profile on Mercier Criterion in Heliotron Plasma: Apr. 2001
- NIFS-693 W. Pei, R. Horiuchi and T. Sato,
Long Time Scale Evolution of Collisionless Driven Reconnection in a Two-Dimensional Open System: Apr. 2001
- NIFS-694 L.N. Vyachenslavov, K. Tanaka, K. Kawahata,
CO₂ Laser Diagnostics for Measurements of the Plasma Density Profile and Plasma Density Fluctuations on LHD Apr. 2001
- NIFS-695 T. Ohkawa,
Spin Dependent Transport in Magnetically Confined Plasma: May 2001
- NIFS-696 M. Yokoyama, K. Ida, H. Sanuki, K. Itoh, K. Narihara, K. Tanaka, K. Kawahata, N. Ohyabu and LHD experimental group
Analysis of Radial Electric Field in LHD towards Improved Confinement: May 2001
- NIFS-697 M. Yokoyama, K. Itoh, S. Okamura, K. Matsuoka, S.-I. Itoh,
Maximum-J Capability in a Quasi-Axisymmetric Stellarator: May 2001
- NIFS-698 S.-I. Itoh and K. Itoh,
Transition in Multiple-scale-lengths Turbulence in Plasmas: May 2001
- NIFS-699 K. Ohi, H. Naitou, Y. Tauchi, O. Fukumasa,
Bifurcation in Asymmetric Plasma Divided by a Magnetic Filter: May 2001
- NIFS-700 H. Miura, T. Hayashi and T. Sato,
Nonlinear Simulation of Resistive Ballooning Modes in Large Helical Device: June 2001
- NIFS-701 G. Kawahara and S. Kida,
A Periodic Motion Embedded in Plane Couette Turbulence: June 2001
- NIFS-702 K. Ohkubo,
Hybrid Modes in a Square Corrugated Waveguide: June 2001
- NIFS-703 S.-I. Itoh and K. Itoh,
Statistical Theory and Transition in Multiple-scale-lengths Turbulence in Plasmas: June 2001